were analyzed by Western blot as described previously [11]. Briefly, tissue was homogenized in lysis buffer containing 25 mM Tris–HCl (pH 7.4), 25 mM NaCl, 0.5 mM EGTA, 10 mM sodium pyrophosphate, 1 mM sodium orthovanadate, 10 mM NaF, 10 nM okadaic acid, 1 mM PMSF, 20 μg/ml aprotinin, and 20 μg/ml leupeptin. Protein concentration was determined using a protein assay kit (Bio-Rad) and equal amounts of total protein (40 μg/lane) were separated on 8% SDS–polyacrylamide gel. Separated proteins were transferred to nitrocellulose membrane (Amersham Life Science). Membranes were incubated with anti-mouse dihydropyridine L-type Ca^{2+} channel α-2 subunit monoclonal antibody (Affinity Bioreagents) or anti-mouse SERCA2 monoclonal antibody (Affinity Bioreagents) at 4 °C overnight. After washing, the membranes were incubated with horseradish peroxidase-conjugated goat anti-mouse antibody for 1 h. Immunoreactive protein was visualized using an enhanced chemiluminescence detection kit (ECL, Amersham).

Ischemia/reperfusion. Hearts were excised from mice and connected to the perfusion cannula via the aorta as described previously [8]. Retrograde perfusion was maintained with Krebs–Henseleit solution. To evaluate the contractile function, a polyethylene film balloon was inserted into the cavity of the left ventricle through the left atrium. The balloon was filled with saline to adjust the baseline end-diastolic pressure to 5–10 mmHg. Hearts were subjected to no-flow, global ischemia by clamping the perfusion line. After 30 min of ischemia, the clamp was released and the hearts were reperfused for 120 min. Left ventricular developed pressure (LVDP) was designated as difference between systolic and diastolic pressures of the left ventricle. After 120 min, the heart was incubated for 5 min at 37 °C in a 1% solution of triphenyltetrazolium chloride (TTC). The sizes of infarcted area (pale) and viable ischemic-reperfused area (red) were measured by computed planimetry (Scion Image 1.62). Infarct size was calculated as described previously [12].

Statistics analysis. All data are presented as means ± SEM. Statistical analyses of the data were performed using Student's *t* test. Probability values less than 0.05 were considered to be significant.

Results

NCX current density and Western blot analysis

We previously reported that the protein content of NCX in NCX KO mice hearts was ~50% of that in WT mice hearts [13]. To elucidate the functional activity, we examined NCX current densities from −40 to 40 mV in WT ($n = 9$) and NCX KO ventricular cells ($n = 6$) (Fig. 1). The densities of the reverse mode of NCX at 40 mV in ventricular cells of KO mice (0.57 ± 0.07 pA/pF) were approximately half (55.4%) compared with those of WT mice (1.04 ± 0.14 pA/pF). These results suggest that the functional activity as well as the protein content of NCX in the myocardium of NCX KO mice is approximately half of those of WT mice.

Western blot analysis revealed that there was no difference in the protein levels of L-type Ca^{2+} channel and SERCA2 between the two groups (data not shown).

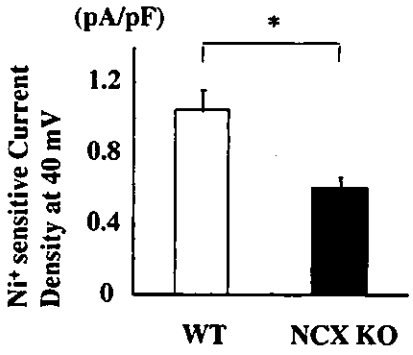

Fig. 1. NCX current densities. The densities of the reverse mode of NCX at 40 mV in ventricular myocytes isolated from WT ($n = 9$) and NCX KO mice hearts ($n = 6$). Values are expressed as means ± SEM. *$p < 0.05$ vs. WT mice.

Mechanical function of hearts before and after ischemia/reperfusion

There were no significant differences in the basal hemodynamic parameters including heart rate, left ventricular pressure, end-diastolic pressure, and positive and negative d*P*/d*t*, between WT and KO mice (Table 1). After ischemia, there was no significant difference between the two groups in several parameters such as time to no beating, time to contracture, and left ventricular end-diastolic pressure (Fig. 2). After reperfusion, however, hearts of KO mice started to beat earlier than those of WT mice (Fig. 2). At 120 min after reperfusion, contractile function (left ventricular developed pressure) of KO mice hearts was significantly better (51.7 ± 12.7% of pre-ischemic value) than that of WT mice hearts (26.3 ± 6.9%, $p < 0.05$) (Fig. 3).

Myocardial infarction after ischemia/reperfusion

After ischemia/reperfusion, there was much viable myocardium in KO hearts than WT hearts (red lesion in Fig. 4A). The infarct size was significantly smaller in KO hearts (32 ± 9%) than in WT hearts (68 ± 10%, $p < 0.05$) (white lesion in Figs. 4A and B).

Table 1
Hemodynamic parameters of NCX KO mice

	WT ($n = 6$)	NCX KO ($n = 7$)
HR(bpm)	356 ± 40	378 ± 77
LVP (mmHg)	142.8 ± 40	146.3 ± 34.5
EDP (mmHg)	4.4 ± 1.5	4.3 ± 1.3
d*P*/d*t* (mmHg/s)	7368 ± 630	7845 ± 2582
−d*P*/d*t* (mmHg/s)	5204 ± 782	5539 ± 1157
Time to no beating (min)	2.2 ± 0.9	2.2 ± 1.6
Time to contracture (min)	6.2 ± 1.7	6.3 ± 2.0
EDP at 25 min (mmHg)	67.3 ± 9.2	63.8 ± 10.8

HR, heart rate; LVP, left ventricular pressure; EDP, LV end-diastolic pressure; d*P*/d*t* and −d*P*/d*t*, positive and negative first derivatives for maximal rates of LV pressure development.

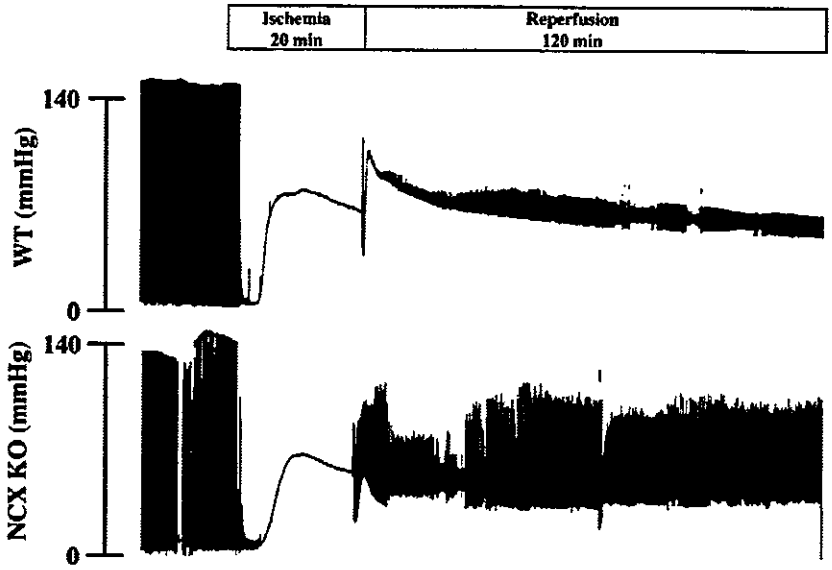

Fig. 2. Ex vivo studies. Changes in LVP during ischemia/reperfusion. Representative LVP records of WT and NCX KO mice hearts are shown. Note that KO mice hearts started to contract earlier than WT mice hearts after reperfusion.

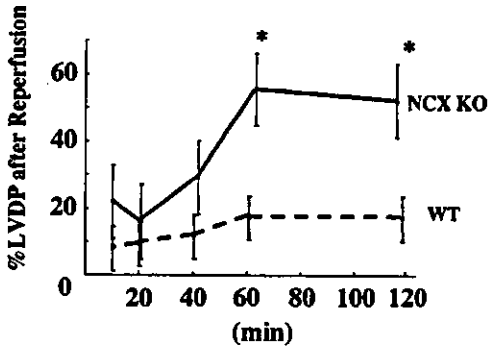

Fig. 3. LVDP of hearts of NCX KO mice ($n = 7$) and WT mice ($n = 6$) hearts after reperfusion. Values are expressed as means ± SEM. $^*p < 0.05$ vs. WT mice.

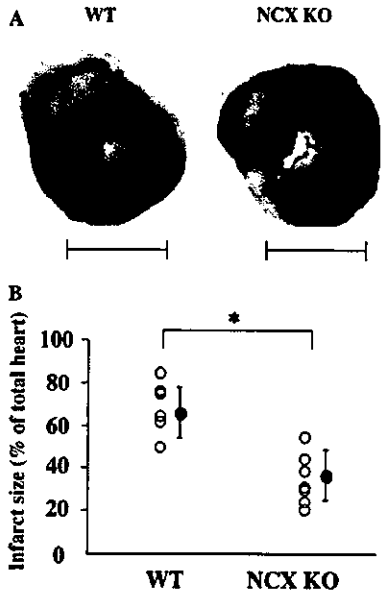

Fig. 4. (A) Representative TTC staining photographs of WT and NCX KO mice hearts after ischemia/reperfusion are shown. Infarcted area is expressed as white lesion and viable myocardium is expressed as red lesion. Bar = 2 mm. (B) Myocardial infarct size is expressed as percentage for total heart of WT mice ($n = 6$) and NCX KO mice ($n = 7$). Values are expressed as means ± SEM. $^*p < 0.05$ vs. WT mice.

Discussion

Myocardial cell injury is induced by a combination of mechanical and chemical stresses during ischemia [14]. Reoxygenation after extended periods of ischemia rapidly induces hypercontracture of cardiomyocytes [15] and aggravates the pre-existing injury [16]. The hypercontracture represents a major cause of acute lethal cell injury in the reperfused myocardium [17,18]. It has been hypothesized that an increase in intracellular Ca^{2+} levels of cardiomyocytes through NCX induces the hypercontracture state after reperfusion but not during ischemia by the mechanism described below [5]. During myocardial ischemia, anaerobic metabolism induces acidosis both inside and outside of cardiomyocytes. The Na^+–H^+ exchanger does not operate at this moment because of no difference in H^+ concentration across the plasma membrane of cardiomyocytes. Reperfusion

restores extracellular acidosis, leading to a disparity in H^+ concentration between inside and outside of cardiomyocytes. The increase in intracellular H^+ concentration activates the Na^+–H^+ exchanger, and the elevated intracellular Na^+ concentration triggers a rise in intracellular Ca^{2+} by the reverse mode of NCX [5]. The excessive Ca^{2+} overload induces the catastrophic hypercontracture of cardiomyocytes. In fact, it has been reported that reduction of Ca^{2+} concentration protects cardiomyocytes against hypercontracture evoked by reoxygenation [19]. In contrast, overexpression of NCX increased ischemia/reperfusion injury in mice [20]. Pharmacological inhibition of reverse mode of NCX protected reperfusion injury in cardiomyocytes [19]. These results suggest that NCX is critically involved in the myocardial ischemia/reperfusion injury, however, NCX inhibitors have been recently reported to be not specific to NCX [6]. Two putative NCX inhibitors, KB-R7943 and SEA0400, depressed the Ca^{2+} transients even in cardiomyocytes of NCX null mice [7]. Although these NCX inhibitors have been reported to suppress the reverse mode but not the forward mode of NCX, the administration of high dose of these inhibitors increased infarct size possibly by inhibition of forward mode of NCX [21]. We here demonstrated an important role of NCX in myocardial ischemia/reperfusion injury by using NCX KO mice. The reverse mode of NCX current in KO mice was decreased to a half of WT mice. Loss of function of NCX is assumed to result in alleviation of Ca^{2+} overload, hypercontracture, and cell death after reperfusion. Our present study clearly indicates that the inhibition of NCX contributes to cardioprotection against myocardial ischemia/reperfusion injury and suggests that specific inhibitors of reverse mode of NCX may be useful to prevent the myocardial ischemia/reperfusion injury.

Acknowledgments

We thank to Y. Reien for the current density analysis and R. Kobayashi, E. Fujita, M. Watanabe, M. Iida, and A. Ohkubo for technical assistance. This work was supported in part by grants from Japanese Ministry of Education, Science, Sports and Culture, and Japan Health Sciences Foundation.

References

[1] D. Schulze, P. Kofuji, R. Hadley, M.S. Kirby, R.S. Kieval, A. Doering, E. Niggli, W.J. Lederer, Sodium/calcium exchanger in heart muscle: molecular biology, cellular function, and its special role in excitation–contraction coupling, Cardiovasc. Res. 27 (1993) 1726–1734.

[2] J.H. Bridge, J.R. Smolley, K.W. Spitzer, The relationship between charge movements associated with I_{Ca} and I_{Na-Ca} in cardiac myocytes, Science 248 (1990) 376–378.

[3] A.G. Kleber, Resting membrane potential, extracellular potassium activity, and intracellular sodium activity during acute global ischemia in isolated perfused guinea pig hearts, Circ. Res. 52 (1983) 442–450.

[4] J.G. Pilitsis, F.G. Diaz, M.H. O'Regan, J.W. Phillis, Inhibition of Na^+/Ca^{2+} exchange by KB-R7943, a novel selective antagonist, attenuates phosphoethanolamine and free fatty acid efflux in rat cerebral cortex during ischemia–reperfusion injury, Brain Res. 916 (2001) 192–198.

[5] B.N. Eigel, R.W. Hadley, Antisense inhibition of Na^+/Ca^{2+} exchange during anoxia/reoxygenation in ventricular myocytes, Am. J. Physiol. Heart Circ. Physiol. 281 (2001) H2184–H2190.

[6] H. Reuter, S.A. Henderson, T. Han, T. Matsuda, A. Baba, R.S. Ross, J.I. Goldhaber, K.D. Philipson, Knockout mice for pharmacological screening: testing the specificity of Na^+/Ca^{2+} exchange inhibitors, Circ. Res. 91 (2002) 90–92.

[7] K. Wakimoto, K. Kobayashi, O.M. Kuro, A. Yao, T. Iwamoto, N. Yanaka, S. Kita, A. Nishida, S. Azuma, Y. Toyoda, K. Omori, H. Imahie, T. Oka, S. Kudoh, O. Kohmoto, Y. Yazaki, M. Shigekawa, Y. Imai, Y. Nabeshima, I. Komuro, Targeted disruption of Na^+/Ca^{2+} exchanger gene leads to cardiomyocyte apoptosis and defects in heartbeat, J. Biol. Chem. 275 (2000) 36991–36998.

[8] M. Suzuki, R.A. Li, T. Miki, H. Uemura, N. Sakamoto, Y. Ohmoto-Sekine, M. Tamagawa, T. Ogura, S. Seino, E. Marban, H. Nakaya, Functional roles of cardiac and vascular ATP-sensitive potassium channels clarified by Kir 6.2-knockout mice, Circ. Res. 88 (2001) 570–577.

[9] Y. Watanabe, J. Kimura, Inhibitory effect of amiodarone on Na^+/Ca^{2+} exchange current in guinea-pig cardiac myocytes, Br. J. Pharmacol. 131 (2000) 80–84.

[10] J. Kimura, S. Miyamae, A. Noma, Identification of sodium–calcium exchange current in single ventricular cells of guinea-pig, J. Physiol. 384 (1987) 199–222.

[11] Y. Zou, I. Komuro, T. Yamazaki, S. Kudoh, H. Uozumi, T. Kadowaki, Y. Yazaki, Both Gs and Gi proteins are critically involved in isoproterenol-induced cardiomyocyte hypertrophy, J. Biol. Chem. 274 (1999) 9760–9770.

[12] M. Suzuki, N. Sasaki, T. Miki, N. Sakamoto, Y. Ohmoto-Sekine, M. Tamagawa, S. Seino, E. Marban, H. Nakaya, Role of sarcolemmal K(ATP) channels in cardioprotection against ischemia/reperfusion injury in mice, J. Clin. Invest. 109 (2002) 509–516.

[13] E. Takimoto, A. Yao, H. Toko, H. Takano, M. Shimoyama, M. Sonoda, K. Wakimoto, T. Takahashi, H. Akazawa, M. Mizukami, T. Nagai, R. Nagai, I. Komuro, Sodium calcium exchanger plays a key role in alteration of cardiac function in response to pressure overload, FASEB J. 16 (2002) 373–378.

[14] H.M. Piper, D. Garcia-Dorland, M. Ovize, A fresh look at reperfusion injury, Cardiovasc. Res. 38 (1998) 291–300.

[15] B. Siegmund, A. Koop, T. Klietz, P. Schwartz, H.M. Piper, Sarcolemmal integrity and metabolic competence of cardiomyocytes under anoxia-reoxygenation, Am. J. Physiol. 258 (1990) H285–H291.

[16] M.D. Stern, A.M. Chien, M.C. Capogrossi, D.J. Pelto, E.G. Lakatta, Direct observation of the "oxygen paradox" in single rat ventricular myocytes, Circ. Res. 56 (1985) 899–903.

[17] J.A. Barrabes, D. Garcia-Dorado, M. Ruiz-Meana, H.M. Piper, J. Solares, M.A. Gonzalez, J. Oliveras, M.P. Herrejon, J. Soler-Soler, Myocardial segment shrinkage during coronary reperfusion in situ. Relation to hypercontracture and myocardial necrosis, Pflugers Arch. 431 (1996) 519–526.

[18] C.E. Ganote, Contraction band necrosis and irreversible myocardial injury, J. Mol. Cell. Cardiol. 15 (1983) 67–73.

[19] C. Schafer, Y. Ladilov, J. Inserte, M. Schafer, S. Haffner, D. Garcia-Dorado, H.M. Piper, Role of the reverse mode of the Na^+/Ca^{2+} exchanger in reoxygenation-induced cardiomyocyte injury, Cardiovasc. Res. 51 (2001) 241–250.

[20] H.R. Cross, L. Lu, C. Steenbergen, K.D. Philipson, E. Murphy, Overexpression of the cardiac Na^+/Ca^{2+} exchanger increases susceptibility to ischemia/reperfusion injury in male, but not female, transgenic mice, Circ. Res. 83 (1998) 1215–1223.

[21] J. Inserte, D. Garcia-Dorado, M. Ruiz-Meana, F. Padilla, J. Barrabes, P. Pina, L. Agullo, H. Piper, J. Soler-Soler, Effect of inhibition of Na^+/Ca^{2+} exchanger at the time of myocardial reperfusion on hypercontracture and cell death, Cardiovasc. Res. 55 (2002) 739.

The EMBO Journal (2004) 23, 212–220 | © 2004 European Molecular Biology Organization | All Rights Reserved 0261-4189/04
www.embojournal.org

THE EMBO JOURNAL

Akt negatively regulates the *in vitro* lifespan of human endothelial cells via a p53/p21-dependent pathway

Hideyuki Miyauchi[1], Tohru Minamino[1], Kaoru Tateno, Takeshige Kunieda, Haruhiro Toko and Issei Komuro*

Department of Cardiovascular Science and Medicine, Chiba University Graduate School of Medicine, Chuo-ku, Chiba, Japan

The signaling pathway of insulin/insulin-like growth factor-1/phosphatidylinositol-3 kinase/Akt is known to regulate longevity as well as resistance to oxidative stress in the nematode *Caenorhabditis elegans*. This regulatory process involves the activity of DAF-16, a forkhead transcription factor. Although reduction-of-function mutations in components of this pathway have been shown to extend the lifespan in organisms ranging from yeast to mice, activation of Akt has been reported to promote proliferation and survival of mammalian cells. Here we show that Akt activity increases along with cellular senescence and that inhibition of Akt extends the lifespan of primary cultured human endothelial cells. Constitutive activation of Akt promotes senescence-like arrest of cell growth via a p53/p21-dependent pathway, and inhibition of forkhead transcription factor FOXO3a by Akt is essential for this growth arrest to occur. FOXO3a influences p53 activity by regulating the level of reactive oxygen species. These findings reveal a novel role of Akt in regulating the cellular lifespan and suggest that the mechanism of longevity is conserved in primary cultured human cells and that Akt-induced senescence may be involved in vascular pathophysiology.

The EMBO Journal (2004) **23**, 212–220. doi:10.1038/sj.emboj.7600045; Published online 8 January 2004
Subject Categories: cell cycle; molecular biology of disease
Keywords: aging; Akt; endothelial cells; senescence

Introduction

Cellular senescence is the limited ability of primary human cells to divide when cultured *in vitro* and is accompanied by a specific set of changes in cell morphology, gene expression and function. These phenotypic changes have been implicated in human aging (Faragher and Kipling, 1998). This hypothesis, the cellular hypothesis of aging, was established by Hayflick (1975) and is supported by evidence that the replicative potential of primary cultured human cells is dependent on donor age and that the growth potential of cultured cells correlates well with the mean maximum lifespan of the species from which the cells are derived (Rohme, 1981), although some conflicting data have been reported (Cristofalo *et al*, 1998). Primary cultured cells obtained from patients with premature aging syndromes, such as Werner syndrome and Bloom syndrome, are known to have a shorter lifespan than the cells from age-matched healthy populations (Rohme, 1981; Thompson and Holliday, 1983), further supporting this hypothesis. Cell division is essential for the survival of multicellular organisms that contain renewable tissues, but also places the organism at the risk of developing cancer. It has been suggested that complex organisms have evolved at least two cellular mechanisms to prevent oncogenic transformation, which are apoptosis and cellular senescence (Campisi, 2001). Accordingly, age-associated diseases could be regarded as a by-product of the tumor suppressor mechanism, cellular senescence (Weinstein and Ciszek, 2002).

Many molecular mechanisms have been suggested to contribute to human aging and its associated diseases. Recent genetic analyses have demonstrated that reduction-of-function mutations in the signaling pathway of insulin/insulin-like growth factor-1 (IGF-1)/phosphatidylinositol-3 kinase (PI3K)/Akt (also known as protein kinase B) extend the longevity of the nematode *Caenorhabditis elegans* (Kenyon *et al*, 1993; Morris *et al*, 1996; Paradis and Ruvkun, 1998; Guarente and Kenyon, 2000; Kenyon, 2001; Lee *et al*, 2001; Lin *et al*, 2001; Longo and Finch, 2003). The forkhead transcription factor DAF-16, which is phosphorylated and thereby inactivated by Akt (Lee *et al*, 2001; Lin *et al*, 2001), plays an essential role in this longevity pathway (Lin *et al*, 1997; Ogg *et al*, 1997). More recently, it has been reported that the genes regulating longevity are conserved in organisms ranging from yeast to mice. Mutation of *Sch9*, which is homologous to *Akt*, extends the lifespan of yeast (Fabrizio *et al*, 2001), and mutations that decrease the activity of the insulin/IGF-1-like pathway increase the longevity of fruit flies (Tatar *et al*, 2001) and mice (Bluher *et al*, 2003; Holzenberger *et al*, 2003). These mutations that extend the lifespan are associated with increased resistance to oxidative stress, which is partly mediated by the increased expression of antioxidant genes (Honda and Honda, 1999; Fabrizio *et al*, 2003; Murphy *et al*, 2003).

In mammalian cells, activation of Akt has been reported to induce proliferation and survival, thereby promoting tumorigenesis (Datta *et al*, 1999; Blume-Jensen and Hunter, 2001; Testa and Bellacosa, 2001). Overexpression of Akt can transform NIH3T3 cells (Cheng *et al*, 1997), while introduction of Akt antisense RNA inhibits the tumorigenic phenotype of cancer cells expressing high levels of Akt (Cheng *et al*, 1996). The mechanisms by which Akt promotes cell proliferation and survival are likely to be multifactorial, because it has been reported to directly phosphorylate several components of the cell cycle machinery as well as the cell death machinery (Datta *et al*, 1999). Akt counteracts the effect of

*Corresponding author. Department of Cardiovascular Science and Medicine, Chiba University Graduate School of Medicine, 1-8-1 Inohana, Chuo-ku, Chiba 260-8670, Japan. Tel.: +81 43 226 2097; Fax: +81 43 226 2557; E-mail: komuro-tky@umin.ac.jp
[1]These authors contributed equally to this work

Received: 25 June 2003; accepted: 25 November 2003; Published online: 8 January 2004

©2004 European Molecular Biology Organization

cyclin-dependent kinase inhibitors on cell cycle progression by modulating their intracellular localization and level of transcription (Medema *et al*, 2000; Shin *et al*, 2002; Viglietto *et al*, 2002; Zhou *et al*, 2001a). Akt also increases the cyclin D1 level by inhibiting its degradation, which is important in the G1/S phase transition (Diehl *et al*, 1998). Moreover, it is known that Akt phosphorylates and inactivates proapoptotic factors such as BAD (Datta *et al*, 1997; del Peso *et al*, 1997) and procaspase-9 (Cardone *et al*, 1998), thereby promoting cell survival. Although these reports have suggested an important role of Akt in human malignancy (Blume-Jensen and Hunter, 2001; Testa and Bellacosa, 2001), it has mainly been examined in immortal cell lines and the impact of Akt activation on the growth and lifespan of primary cultured human cells is unknown.

In the present study, we found that inhibition of Akt could prolong the lifespan of primary cultured human endothelial cells, whereas constitutive activation of Akt promoted senescence-like growth arrest via a p53/p21-dependent pathway. Akt-induced growth arrest was inhibited by a mutated forkhead transcription factor that was resistant to Akt phosphorylation. These findings disclose a novel role of Akt in regulating the lifespan of cells and suggest that the mechanism of longevity is conserved in primary cultured human cells.

Results

Akt activation reduces the lifespan of human endothelial cells

We first investigated whether Akt activity was associated with cellular senescence of primary cultured human endothelial cells. Senescent endothelial cells had higher phospho-Akt levels than young endothelial cells (Figure 1A). To assess the actual role of Akt activity in regulating cellular lifespan, we infected primary cultured human endothelial cells with a retroviral vector encoding either constitutively activated myc-tagged Akt (AktCA) or dominant-negative myc-tagged Akt (AktDN). The empty retroviral vector pLNCX (Mock), encoding a neomycin resistance gene alone, was also transduced into endothelial cells as a control. Infected cells were purified using G418 for 7 days and then recultured until the cells underwent senescence. The 8th day after infection is designated as day 0 in all of the following experiments. Western blot analysis with anti-c-Myc antibody and anti-Akt antibody demonstrated that both AktCA and AktDN proteins were expressed by the endothelial cells, showing an approximately 4- to 8-fold increase of total Akt protein compared to endogenous Akt protein (Figure 1B). Long-term culture studies showed that constitutive activation of Akt significantly shortened the lifespan of the endothelial cells, whereas inhibition of Akt activity delayed senescence compared with mock-infected cells (Figure 1B). Introduction of AktDN influenced cellular lifespan in the late passages, but not in the early passages, suggesting that Akt activity increased with further cell division and thus promoted senescence. Expression of AktCA markedly reduced cell growth by day 7 (Figure 1C). AktCA-transduced endothelial cells were flattened and enlarged, while mock- or AktDN-infected endothelial cells exhibited normal morphology and growth (Figures 1C and D). Senescence-associated β-galactosidase activity was also increased in AktCA-transduced cells (Figure 1D). These changes of the phenotype, which were suggestive of senescence, were observed in various types of endothelial cells including microvascular endothelial cells (Supplementary Figure 1). The same senescence-like changes also occurred in confluent endothelial cells (Supplementary Figure 2). Thus, constitutive activation of Akt induced a senescence-like phenotype in human endothelial cells irrespective of the cell type and growth pattern. To further explore the relationship between Akt activity and cell growth, we isolated clones from AktCA-infected endothelial cells and determined the phospho-Akt level and the cell number on day 30. Clones obtained from mock-infected cell populations could be expanded up to $1\text{–}3 \times 10^6$ cells on average and revealed little Akt activity (Figure 1E, lane 1). In contrast, most of the AktCA-infected clones showed almost complete growth arrest and high levels of phospho-Akt expression (Figure 1E, lanes 5–7). However, some AktCA-infected clones showed low phospho-Akt levels and continued to proliferate (Figure 1E, lanes 2–4). Such proliferating populations may lead to underestimation of the growth inhibitory effect of AktCA in long-term culture experiments. The level of phospho-Akt was inversely correlated with the number of cells on day 30 (Figure 1E, right graph). Thus, we concluded that Akt is a negative regulator of the lifespan of primary cultured human endothelial cells.

Upregulation of p21 is essential for Akt-induced growth arrest

To clarify the mechanism of cell growth arrest induced by activation of Akt, we examined the expression of cell cycle regulatory proteins. Expression of p53 and $p21^{Waf1/Cip1}$, but not $p16^{Ink4a}$, was elevated, while the level of phosphorylated Rb was decreased in AktCA-infected cells compared with mock-infected cells (Figure 2A), suggesting that Akt may induce growth arrest by upregulating p53 and p21. To determine the role of p21 in Akt-induced cell growth arrest, we infected primary cultured mouse embryonic fibroblasts (MEF) derived from *p21*-deficient or wild-type mice with AktCA. Similar to endothelial cells, the growth of wild-type MEF was markedly reduced by activation of Akt compared with mock infection (Figure 2B, $p21^{+/+}$). In contrast, Akt-induced cell growth arrest was restored in *p21*-deficient MEF (Figure 2B, $p21^{-/-}$), suggesting that p21 is essential for Akt-induced growth arrest of these cells. It has been reported that expression of p21 is regulated by p53-dependent or -independent transcriptional mechanisms (el-Deiry *et al*, 1993) as well as protein degradation (Maki and Howley, 1997). To investigate the mechanism by which Akt activation increases p21 expression, we assessed the stability of p21 protein and the extent of *p21* transcription. The half-life of p21 protein did not differ between mock- and AktCA-infected endothelial cells (Figure 2C). Northern blot analysis revealed that the level of *p21* mRNA was significantly increased in Akt-infected cells compared with mock-infected cells (Figure 2D). Activation of Akt enhanced transcription of the luciferase reporter gene controlled by the promoter fragment of the human *p21* gene (Figure 2E), indicating that activation of Akt caused the transcriptional upregulation of p21 expression.

Critical role of p53 transcriptional activity in Akt-induced growth arrest

To ascertain whether Akt activation induces the transcriptional activity of p53, we transfected Akt-infected endothelial

©2004 European Molecular Biology Organization

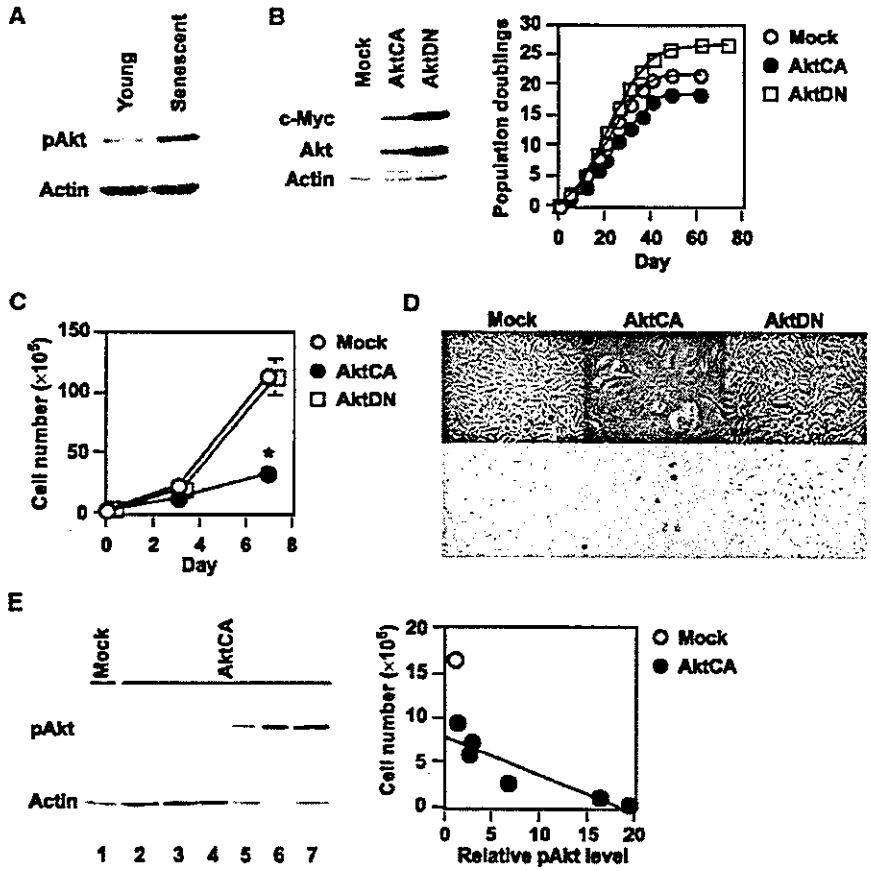

Figure 1 Akt negatively regulates the lifespan of primary cultured human endothelial cells. (**A**) Whole-cell lysates (30 μg) of young (passage 4) or senescent (passages 14–15) human endothelial cells were analyzed for the expression of phospho-Akt (pAkt, Ser473) and actin (loading control) by Western blotting. (**B**) Human endothelial cells were infected with pLNCX (Mock), AktCA or AktDN. After purification, infected cell populations were passaged until they underwent senescence, and the number of cumulative population doublings was determined. Similar results were obtained from three independent experiments. To validate the transduction of AktCA and AktDN, whole-cell lysates (30 μg) of each infected population were examined for the expression of exogenous myc-tagged Akt (c-Myc) and total Akt (Akt). (**C**) Human endothelial cells infected with pLNCX (Mock), AktCA or AktDN were purified with G418 for 7 days and seeded at a density of 3×10^5 cells per 100 mm plate on day 0. Cell number per 100 mm plate was then counted at indicated time points. $^*P<0.001$ versus Mock, ANOVA, $n=4$. (**D**) Cell morphology (upper panel) and senescence-associated β-galactosidase staining (lower panel) in endothelial cells infected with pLNCX (Mock), AktCA or AktDN. (**E**) Independent clones were isolated from pLNCX (Mock)- or AktCA-infected endothelial cells. At 30 days after isolation, the cell number of each clone was counted. Whole-cell lysates (~10 μg) of isolated clones were also prepared and analyzed for the expression of phospho-Akt by Western blotting (left panel, mock-infected clone for lane 1 and AktCA-infected clones for lanes 2–7). The cell number of each clone was as follows: 16.6×10^5 for lane 1; $6–10 \times 10^5$ for lanes 2–4; $0.1–2 \times 10^5$ for lanes 5–7. As the availability of samples was limited in the case of most AktCA-infected clones, the lysates used were less than 10 μg (lanes 5–7). Therefore, the levels of phospho-Akt were standardized on the basis of actin expression, and the relative level of phospho-Akt and the cell number of each clone were plotted in the graph (right panel, $r=0.92$, $P<0.01$). The corrected value of phospho-Akt in mock-infected clones (lane 1) is set at 1.

cells with the luciferase reporter gene containing 13 copies of the p53-binding consensus sequence (PG13). Introduction of AktCA induced *p53* promoter-driven luciferase activity compared with mock infection, but not luciferase activity driven by a promoter containing 15 copies of a similar sequence with mutation at critical positions (MG15) (Figure 3A). To further assess the relation between Akt and p53 transcription activity, we tested whether ablation of p53 could circumvent Akt-induced growth arrest. We infected human endothelial cells with a retroviral vector encoding the E6 oncoprotein of HPV16, which binds p53 and facilitates its destruction by ubiquitin-mediated proteolysis (pBabe E6). We also infected the same cells with the empty vector encoding resistance to puromycin alone (pBabe). Both cell populations were then subjected to infection with pLNCX or AktCA. Activation of Akt markedly inhibited the growth of pBabe-infected endothelial cells (Figure 3B, pBabe), while growth inhibition was completely abolished in E6-infected cells (Figure 3B, E6). Changes of cell morphology were also reversed to normal by introduction of E6 (Figure 3C). Ablation of p53 also lessened the decrease in the lifespan of AktCA-infected cells (Supplementary Figure 3). These results indicate a critical role of p53 in Akt-induced cell growth arrest. Introduction of AktCA did not induce p21 expression in E6-infected cells (Figure 3D), suggesting that constitutive activation of Akt increases induction of the transcription of *p21* by a p53-dependent mechanism and thereby promotes cell growth arrest.

©2004 European Molecular Biology Organization

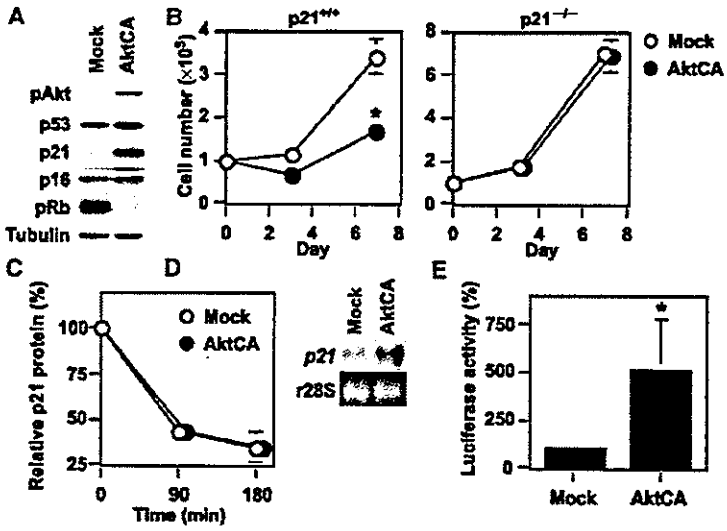

Figure 2 Upregulation of p21 is essential for Akt-induced growth arrest. (**A**) Whole-cell lysates (30 μg) of pLNCX (Mock)- or AktCA-infected endothelial cells on day 0 were examined for the expression of phospho-Akt (pAkt), cell cycle regulatory proteins and tubulin (loading control) by Western blotting. (**B**) MEF derived from wild-type ($p21^{+/+}$) or *p21*-deficient mice ($p21^{-/-}$) were infected with pLNCX (Mock) or AktCA, purified with G418 for 7 days and seeded at a density of 1×10^5 cells per 100 mm plate on day 0. Cell number per 100 mm plate was then counted at indicated time points. $^*P < 0.001$ versus Mock, ANOVA, $n = 4$. (**C**) Human endothelial cells infected with pLNCX (Mock) or AktCA were treated with cycloheximide (10 μg/ml) for the indicated time interval. Whole-cell lysates (30 μg) were then prepared at each time point and assayed for the expression of p21 and actin (loading control) by Western blotting. The graph indicates the results of densitometric analysis for the levels of p21 protein relative to actin expression. The value at time 0 is set at 100%. (**D**) Total RNA (30 μg) was extracted from human endothelial cells infected with pLNCX (Mock) or AktCA and analyzed for *p21* mRNA levels by Northern blotting (upper panel). Ribosomal RNA was used as an internal control (lower panel). (**E**) The luciferase reporter gene plasmid controlled by the promoter of the human *p21* gene was transfected into endothelial cells infected with pLNCX (Mock) or AktCA 24 h before the luciferase activity was measured. The activity in mock-infected cells is set at 100%. $^*P < 0.05$ versus Mock, paired *t*-test, $n = 4$.

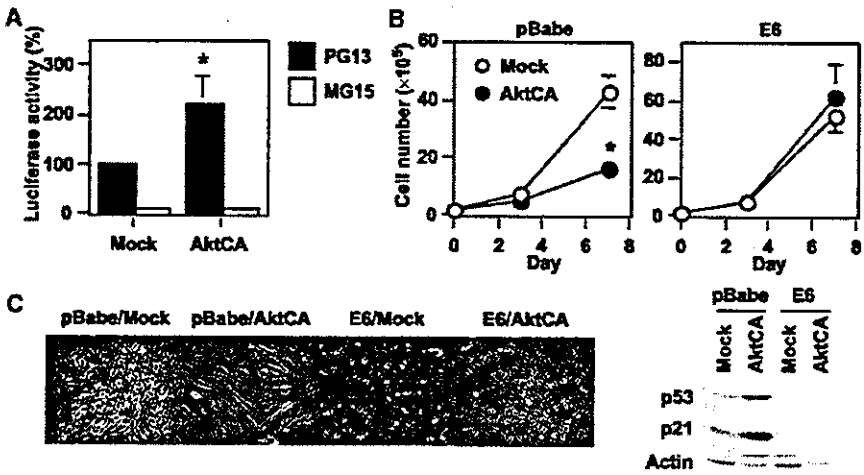

Figure 3 Critical role of p53 transcriptional activity in Akt-induced growth arrest. (**A**) The luciferase reporter gene plasmid pPG13-Luc containing the p53-binding sequence or pMG15-Luc containing the mutated p53-binding sequence was transfected into endothelial cells infected with pLNCX (Mock) or AktCA 24 h before the luciferase activity was measured. The activity of PG13-Luc in mock-infected cells is set at 100%. $^*P < 0.005$ versus Mock, ANOVA, $n = 4$. (**B**) Human endothelial cells were infected with pBabe (empty vector) or pBabe E6 and purified with puromycin. Infected cells were then transduced with pLNCX or AktCA as described in Figure 1C and seeded at a density of 2×10^5 cells per 100 mm plate on day 0. Cell number was then counted at indicated time points. $^*P < 0.05$ versus Mock, ANOVA, $n = 4$. (**C**) Morphology of cell populations prepared in (B). (**D**) Whole-cell lysates (30 μg) were extracted from cells prepared in (B) and examined for the expression of p53, p21 and actin (loading control).

Forkhead transcription factor mediates Akt-induced growth arrest

In *C. elegans*, a reduction-of-function mutation in the PI3K/Akt pathway leads to activation of the forkhead transcription factor DAF-16, resulting in extension of the lifespan, and this effect is inhibited by mutations of antioxidant genes (Murphy *et al*, 2003). Recent evidence indicates that the mammalian forkhead transcription factor FOXO3a (also known as FKHR-L1)

©2004 European Molecular Biology Organization

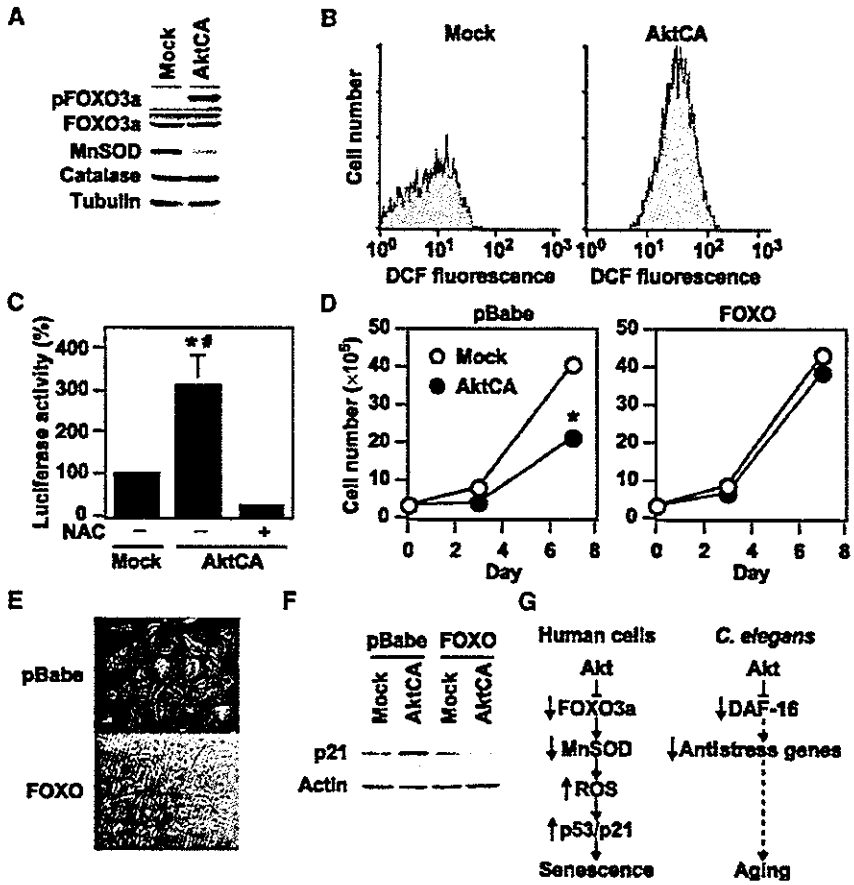

Figure 4 FOXO3a mediates Akt-induced growth arrest via the ROS/p53/p21-dependent mechanisms. (**A**) Whole-cell lysates (30 μg) of pLNCX (Mock)- or AktCA-infected endothelial cells were examined for expression of phospho-FOXO3a (pFOXO3a, Thr32), total FOXO3a (FOXO3a), MnSOD, catalase and tubulin (loading control) by Western blotting. (**B**) Human endothelial cells infected with pLNCX (Mock) or AktCA were loaded with DCF for 30 min and analyzed by FACS. Representative results from two independent experiments are shown. (**C**) The luciferase reporter gene plasmid PG13-Luc was transfected into endothelial cells infected with pLNCX (Mock) or AktCA and cultured in the absence or presence of NAC (0.5 mM). At 24 h after transfection, the luciferase activity was measured. The activity in mock-infected cells is set at 100%. $^{*}P<0.01$ versus Mock, $^{\#}P<0.001$ versus AktCA + NAC, ANOVA, $n=4$. (**D**) Human endothelial cells were infected with pBabe (empty vector) or pBabe mutant FOXO3a (FOXO). Infected cell populations were then transduced with pLNCX (Mock) or AktCA and seeded at a density of 3×10^5 cells per 100 mm plate on day 0. Cell number was then counted at indicated time points. $^{*}P<0.05$ versus Mock, ANOVA, $n=3$. (**E**) Morphology of Akt-infected cell populations prepared in (D). (**F**) Whole-cell lysates (30 μg) prepared in (D) were examined for the expression of p21 and actin (loading control) by Western blotting. Constitutive activation of Akt inhibits the transcriptional activity of FOXO3a and thereby downregulates *MnSOD*, leading to an increase of ROS that promotes senescence-like growth arrest via the p53/p21-dependent pathway. (**G**) Proposed signaling pathway of Akt-induced senescence in human endothelial cells compared with that in *C. elegans*. Akt inactivates FOXO3a and thereby downregulates its target antioxidant gene *MnSOD*, leading to an increase of ROS. ROS induces p53 activity, resulting in upregulation of p21 expression, which promotes cellular senescence in human endothelial cells. In *C. elegans*, the PI3K/Akt pathway also negatively regulates longevity by inactivating DAF-16 activity. This regulatory pathway partly involves the decreased expression of anti-stress genes including *SOD*.

upregulates radical scavenger genes that have a protective effect against oxidative damage in human cells (Kops *et al*, 2002; Nemoto and Finkel, 2002). To investigate the role of FOXO3a in Akt-induced growth arrest, we examined the expression of FOXO3a and antioxidant genes. Phosphorylated FOXO3a (the inactive form) was increased in AktCA-infected endothelial cells compared with mock-infected cells (Figure 4A). The level of manganese superoxide dismutase (MnSOD), but not catalase, was reduced in AktCA-infected endothelial cells (Figure 4A). Consistent with the decreased level of MnSOD, AktCA-infected endothelial cells exhibited an increase of reactive oxygen species (ROS), as assessed using the redox-sensitive fluorophore 2′,7′-dichlorofluorescein diacetate (DCF) (Figure 4B). Since oxidative stress is postulated to induce the activation of p53 (Finkel and Holbrook, 2000), we examined the effect of an ROS scavenger, *N*-acetyl cysteine (NAC), on *p53* promoter activity (PG13) in AktCA-infected endothelial cells. The enhancement of *p53* promoter-driven luciferase activity by AktCA was significantly lessened after treatment with NAC, suggesting that ROS are involved in Akt-induced senescence-like growth arrest (Figure 4C). To further determine the causal link between Akt-induced growth arrest and phosphorylation of FOXO3a, we tested a mutated FOXO3a that was resistant to phosphorylation by Akt. Introduction of this FOXO3a mutant prevented senescence-like growth arrest and cellular morphological changes induced by activation of

©2004 European Molecular Biology Organization

Akt (Figures 4D and E). Moreover, induction of p21 expression by Akt activation was effectively inhibited by the mutant form of FOXO3a (Figure 4F). These results suggest that constitutive activation of Akt inhibits the transcriptional activity of FOXO3a and thereby downregulates *MnSOD*, leading to an increase of ROS that promotes senescence-like growth arrest via the p53/p21-dependent pathway (Figure 4G). This signaling pathway could be recaptured in endothelial cells undergoing replicative senescence (Supplementary Figure 4), which suggests that Akt-induced growth arrest is relevant to physiological senescence and may also be involved in human vasculopathy.

Pathophysiological role of Akt-induced endothelial cell senescence

To investigate whether atherogenic stimuli could activate Akt in human atheroma tissues, we examined Akt activity in coronary arteries obtained at autopsy from patients who had ischemic heart disease. We detected Akt activity in endothelial cells on the surface of coronary atherosclerotic lesions, but not in those of the internal mammary arteries from the same patients, which showed minimal atherosclerotic changes (Figure 5A). To investigate the potential role of Akt-induced endothelial senescence in the pathogenesis of vasculopathy, we examined the effect of Akt on angiogenic activity and the expression of proinflammatory molecules. Tube formation by AktCA-infected endothelial cells was significantly reduced compared with that by mock-infected cells (Figure 5B). In addition, expression of intercellular adhesion molecule (ICAM)-1 was increased in AktCA-infected endothelial cells (Figure 5C). To further explore the role of Akt-induced senescence, we tested the influence of insulin on endothelial cell senescence. Treatment with insulin at a pathological dose caused increases in phospho-FOXO3a and p53 activity (Figures 6A and B), which were comparable to the changes seen in AktCA-infected cells. This increase was inhibited by introduction of AktDN (data not shown), indicating that it was dependent on Akt activity. Insulin induced p53 activity in a dose-dependent manner (Figure 6B). Moreover, continuous incubation with insulin was found to accelerate senescence of human endothelial cells, and this effect was also dose dependent (Figure 6C). Thus, it is conceivable that constitutive activation of Akt by growth factors may promote endothelial cell senescence and thereby contribute to vascular pathophysiology.

Discussion

Our results suggested a critical role of Akt activation in regulating the lifespan of primary cultured human cells in a manner similar to the control of longevity by the PI3K/Akt

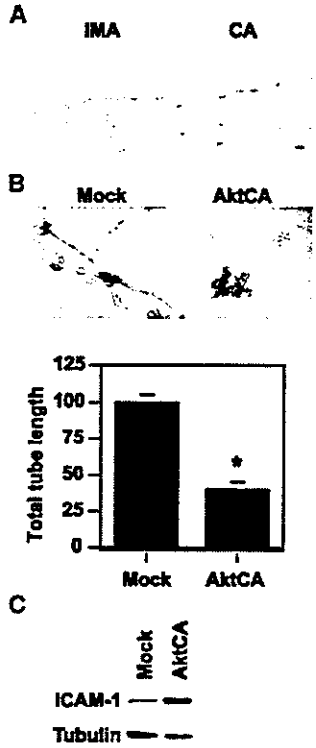

Figure 5 Pathophysiological role of Akt-induced endothelial cell senescence. (**A**) Immunohistochemistry for phospho-Akt (brown) in the coronary arteries (CA) and the internal mammary arteries (IMA) from the same patients. Scale bar: 10 μm. (**B**) Tube formation assay. Human endothelial cells infected with pLNCX (Mock) or AktCA were seeded onto Matrigel. After 48 h, the total tube length was estimated by an angiogenesis image analyzer (Kurabo, Osaka, Japan). The graph shows relative tube length in Mock- and AktCA-infected cells. The length in Mock-infected cells is set at 100%. $^{*}P<0.005$ versus Mock, unpaired *t*-test, $n=4$. (**C**) Whole-cell lysates (30 μg) of pLNCX (Mock)- or AktCA-infected endothelial cells were examined for the expression of ICAM-1 and tubulin (loading control) by Western blotting.

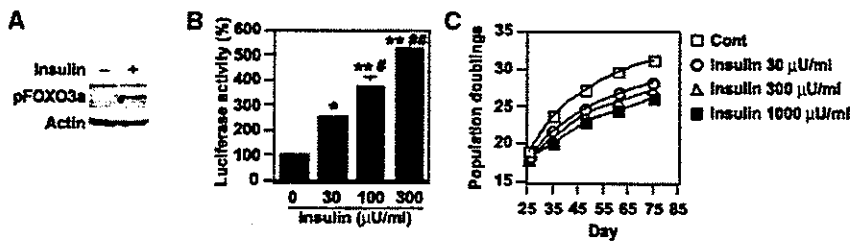

Figure 6 Insulin promotes endothelial cell senescence. (**A**) Whole-cell lysates (30 μg) of human endothelial cells treated with insulin (1000 μU/ml) for 30 min were analyzed for the levels of phosphorylated FOXO3a and actin (loading control) by Western blotting. (**B**) The luciferase reporter gene plasmid PG13-Luc was transfected into endothelial cells in the presence of insulin at the indicated dose. At 24 h after transfection, the luciferase activity was measured. The activity in controls is set at 100%. $^{*}P<0.05$, $^{**}P<0.0001$ versus control, $^{\#}P<0.01$, $^{\#\#}P<0.001$ versus insulin 30 μU/ml, $n=4$. (**C**) Human endothelial cells were cultured in the presence of insulin at the indicated dose and passaged. The number of cumulative population doublings was determined ($n=3$).

©2004 European Molecular Biology Organization

signaling pathway in *C. elegans*. We have previously demonstrated that senescent endothelial cells are present in human atherosclerotic plaques, but not nonatherosclerotic lesions, and express high levels of proinflammatory molecules that are known to promote atherogenesis (Minamino *et al*, 2002). Since Akt is known to be activated by various atherogenic stimuli (Cantley, 2002), our findings imply that constitutive activation of Akt by atherogenic stimuli may induce endothelial cell senescence in atheroma tissue and thereby contribute to atherogenesis. Consistent with this hypothesis, we observed that Akt was phosphorylated in human atheroma but not in normal arteries, and that expression of proinflammatory molecules was increased in AktCA-infected endothelial cells compared with mock-infected cells. Moreover, insulin increased p53 activity via an Akt-dependent mechanism and reduced the lifespan of endothelial cells. Thus, an Akt-induced senescence-like phenotype may be particularly involved in diabetic vasculopathy, since hyperinsulinemia could constitutively activate Akt in endothelial cells.

Although one supposes that Akt-induced senescence might be an artifact, the following points suggest that our findings are valid. First, we observed that Akt activity was increased in endothelial cells undergoing replicative senescence and that inhibition of this endogenous increase in Akt activity by AktDN led to prolongation of the cellular lifespan. This is compatible with many earlier studies demonstrating that reduction-of-function mutations in the insulin/PI3K/Akt pathway extend longevity in organisms ranging from yeast to mice (Longo and Finch, 2003). This signaling pathway (including phosphorylation of FOXO3a and downregulation of MnSOD induced by Akt) could be recaptured in endothelial cells undergoing replicative senescence (Supplementary Figure 4), which suggests that Akt-induced growth arrest may be relevant to physiological senescence. Second, we found that growth was significantly decreased in cloned populations obtained from cells infected with AktCA that exhibited a moderate increase in Akt activity (Figure 1, lanes 2–4). The level of Akt activity in these cells was similar to that in endothelial cells undergoing replicative senescence, suggesting that a physiological level of Akt activation may be able to promote cellular senescence. Third, we found that phospho-FOXO3a levels in AktCA-infected cells were comparable to those in endothelial cells stimulated by insulin at the level seen in patients with type II diabetes. The p53 transcriptional activity in AktCA-infected cells was also similar to that of cells treated with insulin. These results indicate that the pathophysiological activation of Akt was mimicked by infection with AktCA.

Gain-of-function mutations in the PI3K/Akt signaling pathway are frequently found in human cancers (Testa and Bellacosa, 2001). Thus, Akt-induced growth arrest may be another antitumorigenesis mechanism similar to Ras-induced senescence (Serrano *et al*, 1997; Campisi, 2001; Wright and Shay, 2001). We found that ablation of p53 prevented Akt-induced growth arrest, whereas both the p53- and p16-dependent pathways are reported to be essential for Ras-induced senescence (Serrano *et al*, 1997; Lin *et al*, 1998). Oncogenic Ras also induced premature senescence of primary cultured human vascular cells, which was suppressed by inhibition of mitogen-activated protein kinase kinase but not PI3K (Minamino *et al*, 2003), suggesting that Akt-induced growth arrest may be distinct from Ras-induced senescence. A recent study demonstrated that senescent cells could potentiate the oncogenic transformation of nearby normal cells (Krtolica *et al*, 2001), which suggests that induction of senescence by Akt as well as Ras may actually be pro-oncogenic.

We found that Akt increased the transcriptional activity of p53, resulting in upregulation of *p21* in primary cultured human endothelial cells. Our results are consistent with previous reports that Akt mediates induction of p21 expression by various stimuli in myoblasts and vascular cells (Lawlor and Rotwein, 2000a, b; Schonherr *et al*, 2001). However, Akt is also reported to induce cytoplasmic localization of p21 (Zhou *et al*, 2001a), thereby promoting cell proliferation, and to promote nuclear translocation of Mdm2 (a negative regulator of p53), leading to a reduction of both p53 levels and transactivation (Mayo and Donner, 2001; Zhou *et al*, 2001b). Such changes were not observed in human endothelial cells (H Miyauchi, unpublished data). It is noteworthy that most other studies have examined immortal cells, in which the normal cell cycle machinery might be impaired, and the effects of constitutive Akt activation have not been explored. Although the effects of tissue-specific transgenic expression of constitutively activated *Akt* alleles have been reported in several different murine models, most of these animals do not develop tumors (Vivanco and Sawyers, 2002), suggesting that activation of Akt is insufficient to cause cancer unless combined with other oncogenic stimuli. Thus, like Ras, Akt may promote cell proliferation and survival or senescence-like growth arrest, depending on various factors including the cellular context as well as the duration and extent of its activation.

In conclusion, we found that Akt negatively regulates the lifespan of primary cultured human endothelial cells via the p53/p21-dependent pathway, and this action is mediated at least partly by the forkhead transcription factor that regulates cellular ROS levels. Our data not only support the previous findings about the signaling pathway for longevity in *C. elegans*, but also provide a novel insight for research on the treatments of human vasculopathy and cancer.

Materials and methods

Cell culture

Human aortic endothelial cells, human dermal microvascular endothelial cells and human umbilical vein endothelial cells were purchased from Bio Whittaker (Walkersville, MD), and cultured according to the manufacturer's instructions. These cells gave similar results (data not shown). We defined senescent cells as the cultures that do not increase in the cell number and remain subconfluent for 2 weeks. We confirmed the senescent phenotype with SA-β-gal activity assay. Wild-type and *p21*-deficient MEFs were prepared from day 13.5 embryos derived from crosses between $p21^{+/-}$ mice (Jackson, Bar Harbor, ME) and cultured in DMEM plus 10% fetal bovine serum. Senescence-associated β-galactosidase staining was performed as described (Minamino *et al*, 2002). Tube formation assay was performed according to the manufacturer's instructions (BioCoat Angiogenesis System, Clontech, Palo Alto, CA).

Retroviral infection

The following plasmids were used for generating retroviruses: pLNCX (Clontech, Palo Alto, CA) and pBabe (a gift from Dr CW Lowe, Cold Spring Harbor Laboratory, Cold Spring Harbor, NY). We created the pLNCX-based vector expressing a constitutively active form of Akt (AktCA) or a dominant-negative form of Akt (AktDN) by using the fragment derived from the plasmid pBS-CA-Akt or

©2004 European Molecular Biology Organization

pBS-DN-Akt (Fujishiro *et al*, 2001), respectively (a gift from Dr T Asano, Tokyo University, Tokyo, Japan). The pBabe-based vector expressing a mutant form of FOXO3a was constructed by using the fragment derived from pECE FOXO3aTM (Brunet *et al*, 1999) (a gift from Dr ME Greenberg, Harvard Medical School, Boston, MA). We also constructed the pBabe-based vector expressing E6 (pBabe E6). Details of the construct are available upon request. Retroviral stocks were generated by transient transfection of packaging cell line (PT67, Clontech) and stored at −80°C until use. Human endothelial cells (passage 4–6) were plated at 5×10^5 cells per 100-mm-diameter dish 24 h before infections. For infections, the culture medium was replaced by retroviral stocks supplemented with 8 μg/ml polybrene (Sigma, Tokyo, Japan). At 48 h after infections, the infected cell populations were selected by culture in 500 μg/ml G418 for 7 days (pLNCX-based vectors). After selection, $1–3 \times 10^5$ cells were seeded onto 100-mm-diameter dishes on the 8th day postinfection. The 8th day after infection is designated as day 0. For double infection, endothelial cells were infected with pBabe, pBabe FOXO3a or pBabe E6 purified with 0.8 μg/ml puromycin for 4 days and subjected to the second infection as described above.

Western blotting and antibodies

Whole-cell lysates (30 μg) were resolved by SDS polyacrylamide gel electrophoresis (PAGE). Proteins were transferred onto a polyvinylidene difluoride (PVDF) membrane (Millipore, Bedford, MA) and incubated with the first antibody followed by an anti-rabbit immunoglobulin G–horseradish peroxidase antibody or anti-mouse immunoglobulin G–horseradish peroxidase antibody (Jackson, West Grove, PA). Specific proteins were detected using enhanced chemiluminescence (Amersham, Tokyo, Japan). The first antibodies used for Western blotting are as follows: antibodies to Akt, p53, ICAM-1, actin and tubulin (Santa Cruz, Santa Cruz, CA); antibodies to retinoblastoma protein and p16 (Pharmingen, Tokyo, Japan); anti-p21 antibody (Oncogene, Cambridge, MA); anti-phospho-Akt (Ser473) antibody (Cell Signaling, Beverly, MA); anti-catalase antibody (Sigma); antibodies to FOXO3a, phospho-FOXO3a (Thr32) and MnSOD (Upstate Biotechnology, Lake Placid, NY).

Northern blotting

Total RNA (30 μg) was extracted using RNA zol B (Tel Test, Friendswood, TX) according to the manufacturer's instructions, separated on a formaldehyde denaturing gel and transferred to a nylon membrane (Amersham). The blot was then hybridized with radiolabeled p21 cDNA probes using the Quickhyb hybridization solution (Stratagene, Tokyo, Japan) according to the manufacturer's instructions.

Luciferase assays

The reporter gene plasmid (1 μg) was transfected into endothelial cells infected with pLNCX (Mock) or AktCA 24 h before luciferase assay. The control vector encoding *Renilla* luciferase (0.1 μg) was co-transfected for an internal control. Luciferase assay was carried out using a dual-luciferase reporter assay system (Promega, Madison, WI) according to the manufacturer's instructions. The plasmids pPG13-Luc, pPG15-Luc and pWWP-LUC-1 (el-Deiry *et al*, 1993) were a gift from Dr B Vogelstein (Johns Hopkins University, Baltimore, MD).

Tissue specimens and histology

Human coronary arteries and internal mammary arteries were obtained from four autopsied individuals who had ischemic heart disease. For immunohistochemistry, the frozen sections (6 μm) were treated with 0.3% hydrogen peroxide in methanol for 20 min, preincubated with 5% goat serum and then treated with anti-phospho-Akt antibody (1:100; Santa Cruz, Santa Cruz, CA) for 1 h at 37°C. Next, the sections were incubated with a biotinylated goat secondary antibody, treated with the avidin–biotin complex (Elite ABC kit, Vector, Burlingame, CA) and stained with diaminobenzidine tetrahydrochloride and hydrogen peroxide. To verify the specificity of the first antibodies, we performed a control staining with nonimmune IgG and excluded the possibility of nonspecific signals. The studies on human samples were approved by our institutional review board.

Statistical analysis

All values were expressed as mean ± s.e.m. Comparison of results between different groups was performed by one-way analysis of variance, paired *t*-test and unpaired *t*-test using StatView 4.5 (Abacus Concepts, Berkeley, CA).

Supplementary data

Supplementary data are available at *The EMBO Journal* Online.

Acknowledgements

We thank Dr B Vogelstein, SW Lowe, ME Greenberg and T Asano for reagents. This work was supported by grants from Takeda Medical Research Foundation, Takeda Science Foundation, Japan Heart Foundation, Mochida Memorial Foundation, Uehara Memorial Foundation, Mitsubishi Pharma Research Foundation and the Ministry of Education, Science, Sports, and Culture of Japan (to TM and IK).

Competing interests statement

The authors declare that they have no competing financial interests.

References

Bluher M, Kahn BB, Kahn CR (2003) Extended longevity in mice lacking the insulin receptor in adipose tissue. *Science* **299:** 572–574

Blume-Jensen P, Hunter T (2001) Oncogenic kinase signalling. *Nature* **411:** 355–365

Brunet A, Bonni A, Zigmond MJ, Lin MZ, Juo P, Hu LS, Anderson MJ, Arden KC, Blenis J, Greenberg ME (1999) Akt promotes cell survival by phosphorylating and inhibiting a Forkhead transcription factor. *Cell* **96:** 857–868

Campisi J (2001) Cellular senescence as a tumor-suppressor mechanism. *Trends Cell Biol* **11:** S27–S31

Cantley LC (2002) The phosphoinositide 3-kinase pathway. *Science* **296:** 1655–1657

Cardone MH, Roy N, Stennicke HR, Salvesen GS, Franke TF, Stanbridge E, Frisch S, Reed JC (1998) Regulation of cell death protease caspase-9 by phosphorylation. *Science* **282:** 1318–1321

Cheng JQ, Altomare DA, Klein MA, Lee WC, Kruh GD, Lissy NA, Testa JR (1997) Transforming activity and mitosis-related expression of the AKT2 oncogene: evidence suggesting a link between cell cycle regulation and oncogenesis. *Oncogene* **14:** 2793–2801

Cheng JQ, Ruggeri B, Klein WM, Sonoda G, Altomare DA, Watson DK, Testa JR (1996) Amplification of AKT2 in human pancreatic cells and inhibition of AKT2 expression and tumorigenicity by antisense RNA. *Proc Natl Acad Sci USA* **93:** 3636–3641

Cristofalo VJ, Allen RG, Pignolo RJ, Martin BG, Beck JC (1998) Relationship between donor age and the replicative lifespan of human cells in culture: a reevaluation. *Proc Natl Acad Sci USA* **95:** 10614–10619

Datta SR, Brunet A, Greenberg ME (1999) Cellular survival: a play in three Akts. *Genes Dev* **13:** 2905–2927

Datta SR, Dudek H, Tao X, Masters S, Fu H, Gotoh Y, Greenberg ME (1997) Akt phosphorylation of BAD couples survival signals to the cell-intrinsic death machinery. *Cell* **91:** 231–241

del Peso L, Gonzalez-Garcia M, Page C, Herrera R, Nunez G (1997) Interleukin-3-induced phosphorylation of BAD through the protein kinase Akt. *Science* **278:** 687–689

Diehl JA, Cheng M, Roussel MF, Sherr CJ (1998) Glycogen synthase kinase-3beta regulates cyclin D1 proteolysis and subcellular localization. *Genes Dev* **12:** 3499–3511

el-Deiry WS, Tokino T, Velculescu VE, Levy DB, Parsons R, Trent JM, Lin D, Mercer WE, Kinzler KW, Vogelstein B (1993) WAF1, a potential mediator of p53 tumor suppression. *Cell* **75:** 817–825

Fabrizio P, Liou LL, Moy VN, Diaspro A, SelverstoneValentine J, Gralla EB, Longo VD (2003) SOD2 functions downstream of Sch9 to extend longevity in yeast. *Genetics* **163:** 35–46

Fabrizio P, Pozza F, Pletcher SD, Gendron CM, Longo VD (2001) Regulation of longevity and stress resistance by Sch9 in yeast. *Science* **292:** 288–290

©2004 European Molecular Biology Organization

Faragher RG, Kipling D (1998) How might replicative senescence contribute to human ageing? *BioEssays* **20:** 985–991
Finkel T, Holbrook NJ (2000) Oxidants, oxidative stress and the biology of ageing. *Nature* **408:** 239–247
Fujishiro M, Gotoh Y, Katagiri H, Sakoda H, Ogihara T, Anai M, Onishi Y, Ono H, Funaki M, Inukai K, Fukushima Y, Kikuchi M, Oka Y, Asano T (2001) MKK6/3 and p38 MAPK pathway activation is not necessary for insulin-induced glucose uptake but regulates glucose transporter expression. *J Biol Chem* **276:** 19800–19806
Guarente L, Kenyon C (2000) Genetic pathways that regulate ageing in model organisms. *Nature* **408:** 255–262
Hayflick L (1975) Current theories of biological aging. *Fed Proc* **34:** 9–13
Holzenberger M, Dupont J, Ducos B, Leneuve P, Geloen A, Even PC, Cervera P, Le Bouc Y (2003) IGF-1 receptor regulates lifespan and resistance to oxidative stress in mice. *Nature* **421:** 182–187
Honda Y, Honda S (1999) The daf-2 gene network for longevity regulates oxidative stress resistance and Mn-superoxide dismutase gene expression in *Caenorhabditis elegans*. *FASEB J* **13:** 1385–1393
Kenyon C (2001) A conserved regulatory system for aging. *Cell* **105:** 165–168
Kenyon C, Chang J, Gensch E, Rudner A, Tabtiang R (1993) A *C. elegans* mutant that lives twice as long as wild type. *Nature* **366:** 461–464
Kops GJ, Dansen TB, Polderman PE, Saarloos I, Wirtz KW, Coffer PJ, Huang TT, Bos JL, Medema RH, Burgering BM (2002) Forkhead transcription factor FOXO3a protects quiescent cells from oxidative stress. *Nature* **419:** 316–321
Krtolica A, Parrinello S, Lockett S, Desprez PY, Campisi J (2001) Senescent fibroblasts promote epithelial cell growth and tumorigenesis: a link between cancer and aging. *Proc Natl Acad Sci USA* **98:** 12072–12077
Lawlor MA, Rotwein P (2000a) Coordinate control of muscle cell survival by distinct insulin-like growth factor activated signaling pathways. *J Cell Biol* **151:** 1131–1140
Lawlor MA, Rotwein P (2000b) Insulin-like growth factor-mediated muscle cell survival: central roles for Akt and cyclin-dependent kinase inhibitor p21. *Mol Cell Biol* **20:** 8983–8995
Lee RY, Hench J, Ruvkun G (2001) Regulation of *C. elegans* DAF-16 and its human ortholog FKHRL1 by the daf-2 insulin-like signaling pathway. *Curr Biol* **11:** 1950–1957
Lin AW, Barradas M, Stone JC, van Aelst L, Serrano M, Lowe SW (1998) Premature senescence involving p53 and p16 is activated in response to constitutive MEK/MAPK mitogenic signaling. *Genes Dev* **12:** 3008–3019
Lin K, Dorman JB, Rodan A, Kenyon C (1997) daf-16: An HNF-3/forkhead family member that can function to double the life-span of *Caenorhabditis elegans*. *Science* **278:** 1319–1322
Lin K, Hsin H, Libina N, Kenyon C (2001) Regulation of the *Caenorhabditis elegans* longevity protein DAF-16 by insulin/IGF-1 and germline signaling. *Nat Genet* **28:** 139–145
Longo VD, Finch CE (2003) Evolutionary medicine: from dwarf model systems to healthy centenarians? *Science* **299:** 1342–1346
Maki CG, Howley PM (1997) Ubiquitination of p53 and p21 is differentially affected by ionizing and UV radiation. *Mol Cell Biol* **17:** 355–363
Mayo LD, Donner DB (2001) A phosphatidylinositol 3-kinase/Akt pathway promotes translocation of Mdm2 from the cytoplasm to the nucleus. *Proc Natl Acad Sci USA* **98:** 11598–11603
Medema RH, Kops GJ, Bos JL, Burgering BM (2000) AFX-like Forkhead transcription factors mediate cell-cycle regulation by Ras and PKB through p27kip1. *Nature* **404:** 782–787
Minamino T, Miyauchi H, Yoshida T, Ishida Y, Yoshida H, Komuro I (2002) Endothelial cell senescence in human atherosclerosis: role of telomere in endothelial dysfunction. *Circulation* **105:** 1541–1544
Minamino T, Yoshida T, Tateno K, Miyauchi H, Zou Y, Toko H, Komuro I (2003) Ras-induced vascular smooth muscle cell senescence in human atherosclerosis. *Circulation* **108:** 2264–2269
Morris JZ, Tissenbaum HA, Ruvkun G (1996) A phosphatidylinositol-3-OH kinase family member regulating longevity and diapause in *Caenorhabditis elegans*. *Nature* **382:** 536–539
Murphy CT, McCarroll SA, Bargmann CI, Fraser A, Kamath RS, Ahringer J, Li H, Kenyon C (2003) Genes that act downstream of DAF-16 to influence the lifespan of *Caenorhabditis elegans*. *Nature* **424:** 277–283
Nemoto S, Finkel T (2002) Redox regulation of forkhead proteins through a p66shc-dependent signaling pathway. *Science* **295:** 2450–2452
Ogg S, Paradis S, Gottlieb S, Patterson GI, Lee L, Tissenbaum HA, Ruvkun G (1997) The Fork head transcription factor DAF-16 transduces insulin-like metabolic and longevity signals in *C. elegans*. *Nature* **389:** 994–999
Paradis S, Ruvkun G (1998) *Caenorhabditis elegans* Akt/PKB transduces insulin receptor-like signals from AGE-1 PI3 kinase to the DAF-16 transcription factor. *Genes Dev* **12:** 2488–2498
Rohme D (1981) Evidence for a relationship between longevity of mammalian species and life spans of normal fibroblasts *in vitro* and erythrocytes *in vivo*. *Proc Natl Acad Sci USA* **78:** 5009–5013
Schonherr E, Levkau B, Schaefer L, Kresse H, Walsh K (2001) Decorin-mediated signal transduction in endothelial cells. Involvement of Akt/protein kinase B in up-regulation of p21(WAF1/CIP1) but not p27(KIP1). *J Biol Chem* **276:** 40687–40692
Serrano M, Lin AW, McCurrach ME, Beach D, Lowe SW (1997) Oncogenic ras provokes premature cell senescence associated with accumulation of p53 and p16INK4a. *Cell* **88:** 593–602
Shin I, Yakes FM, Rojo F, Shin NY, Bakin AV, Baselga J, Arteaga CL (2002) PKB/Akt mediates cell-cycle progression by phosphorylation of p27(Kip1) at threonine 157 and modulation of its cellular localization. *Nat Med* **8:** 1145–1152
Tatar M, Kopelman A, Epstein D, Tu MP, Yin CM, Garofalo RS (2001) A mutant *Drosophila* insulin receptor homolog that extends life-span and impairs neuroendocrine function. *Science* **292:** 107–110
Testa JR, Bellacosa A (2001) AKT plays a central role in tumorigenesis. *Proc Natl Acad Sci USA* **98:** 10983–10985
Thompson KV, Holliday R (1983) Genetic effects on the longevity of cultured human fibroblasts. II. DNA repair deficient syndromes. *Gerontology* **29:** 83–88
Viglietto G, Motti ML, Bruni P, Melillo RM, D'Alessio A, Califano D, Vinci F, Chiappetta G, Tsichlis P, Bellacosa A, Fusco A, Santoro M (2002) Cytoplasmic relocalization and inhibition of the cyclin-dependent kinase inhibitor p27(Kip1) by PKB/Akt-mediated phosphorylation in breast cancer. *Nat Med* **8:** 1136–1144
Vivanco I, Sawyers CL (2002) The phosphatidylinositol 3-Kinase AKT pathway in human cancer. *Nat Rev Cancer* **2:** 489–501
Weinstein BS, Ciszek D (2002) The reserve-capacity hypothesis: evolutionary origins and modern implications of the trade-off between tumor-suppression and tissue-repair. *Exp Gerontol* **37:** 615–627
Wright WE, Shay JW (2001) Cellular senescence as a tumor-protection mechanism: the essential role of counting. *Curr Opin Genet Dev* **11:** 98–103
Zhou BP, Liao Y, Xia W, Spohn B, Lee MH, Hung MC (2001a) Cytoplasmic localization of p21Cip1/WAF1 by Akt-induced phosphorylation in HER-2/neu-overexpressing cells. *Nat Cell Biol* **3:** 245–252
Zhou BP, Liao Y, Xia W, Zou Y, Spohn B, Hung MC (2001b) HER-2/neu induces p53 ubiquitination via Akt-mediated MDM2 phosphorylation. *Nat Cell Biol* **3:** 973–982

©2004 European Molecular Biology Organization

THE JOURNAL OF BIOLOGICAL CHEMISTRY
Vol. 279, No. 12, Issue of March 19, pp. 11384–11391, 2004
Printed in U.S.A.
© 2004 by The American Society for Biochemistry and Molecular Biology, Inc.

Adult Cardiac Sca-1-positive Cells Differentiate into Beating Cardiomyocytes*[S]

Received for publication, October 1, 2003, and in revised form, December 16, 2003
Published, JBC Papers in Press, December 31, 2003, DOI 10.1074/jbc.M310822200

Katsuhisa Matsuura‡§, Toshio Nagai‡, Nobuhiro Nishigaki‡¶, Tomomi Oyama‡, Junichiro Nishi‡, Hiroshi Wada‡, Masanori Sano‡, Haruhiro Toko‡, Hiroshi Akazawa‡, Toshiaki Sato‖, Haruaki Nakaya‖, Hiroshi Kasanuki§, and Issei Komuro‡**

From the ‡Department of Cardiovascular Science and Medicine, Chiba University Graduate School of Medicine, Chiba 260-8670, Japan, the §Department of Cardiology, The Heart Institute of Japan, Tokyo Women's Medical University, Tokyo 162-0054, Japan, the ¶Takeda Chemical Industries, LTD, Osaka 540-8645, Japan, and the ‖Department of Pharmacology, Chiba University Graduate School of Medicine, Chiba 260-8670, Japan

Although somatic stem cells have been reported to exist in various adult organs, there have been few reports concerning stem cells in the heart. We here demonstrate that Sca-1-positive (Sca-1+) cells in adult hearts have some of the features of stem cells. Sca-1+ cells were isolated from adult murine hearts by a magnetic cell sorting system and cultured on gelatin-coated dishes. A fraction of Sca-1+ cells stuck to the culture dish and proliferated slowly. When treated with oxytocin, Sca-1+ cells expressed genes of cardiac transcription factors and contractile proteins and showed sarcomeric structure and spontaneous beating. Isoproterenol treatment increased the beating rate, which was accompanied by the intracellular Ca^{2+} transients. The cardiac Sca-1+ cells expressed oxytocin receptor mRNA, and the expression was up-regulated after oxytocin treatment. Some of the Sca-1+ cells expressed alkaline phosphatase after osteogenic induction and were stained with Oil-Red O after adipogenic induction. These results suggest that Sca-1+ cells in the adult murine heart have potential as stem cells and may contribute to the regeneration of injured hearts.

The heart has long been thought to adapt to increased work and loss of cardiomyocytes by the cellular hypertrophy of residual cardiomyocytes, but not by the proliferation of mature cardiomyocytes or the differentiation of undifferentiated cells. However, recent reports have suggested that adult cardiomyocytes can proliferate under certain pathologic conditions and that there are cells expressing stem cell markers in the adult heart (1–4). It has been reported that Sca-1- and c-kit-positive (+) cells exist in the adult heart (5) and that adult murine hearts contain potential stem cells; side population (SP)[1] cells (6, 7). However, it remains to be clarified whether these cells have the characteristics of stem cells such as abilities of self-renewal and differentiation into various types of cells including mature cardiomyocytes.

Sca-1 is a member of the Ly-6 family and has first reported as one of the cell surface markers of hematopoietic stem cells (8). Recently many reports have demonstrated that multipotential stem cells derived from bone marrow and skeletal muscle express Sca-1. Okumoto *et al.* (9) have reported that Sca-1+ cells from bone marrow differentiate into hepatocyte when treated with hepatic growth factor. Gojo *et al.* (10) have reported that adult mesenchymal stem cells from bone marrow abundantly express Sca-1 and differentiate into cardiomyocyte *in vivo*. Qu-Petersen *et al.* (11) have shown that skeletal muscle-derived stem cells, which highly express Sca-1, contribute to the regeneration of the skeletal muscle in a mouse model of Duchenne muscle dystrophy. They also demonstrated that the skeletal muscle-derived stem cells were able to differentiate into neural cells and endothelial cells. Asakura *et al.* (12) have reported that ~90% of SP cells in skeletal muscle express Sca-1. It has been reported that skeletal muscle-derived Sca-1+ and CD34+ cells restore dystrophin in mdx mice (13) and that CD34+ and CD45− cells in the interstitial spaces of skeletal muscle, which highly express Sca-1, differentiate into adipocytes, endothelial, and myogenic cells (14). These findings suggest that Sca-1 might be important evidence for somatic stem cells.

Currently little is known about the humoral or growth factors that induce cardiomyogenic differentiation. It has been shown that ectopic application of bone morphological protein (BMP) 2 and 4 elicits cardiogenic responses in the chick *in vivo* system (15), and fibroblast growth factor (FGF) 2 and 4, combined with BMP-2 or BMP-4 can induce cardiogenesis in chick non-precardiac mesoderm (16). The non-canonical Wnt/c-Jun-N-terminal kinase pathways have been reported to be essential for cardiac induction in frog and chick embryo systems (17, 18). These factors are prerequisites for early cardiac differentiation but are not sufficient for accomplishing differentiation into mature beating cardiomyocytes. Recently Paquin *et al.* (19) have reported that oxytocin induces differentiation of P19 embryonic carcinoma cells to beating cardiomyocytes. In support of the role of oxytocin in cardiac development, the oxytocin receptor is increased at the protein level in the murine heart from day 7 of gestation, when cardiac differentiation starts

* This study was supported by a grant-in-aid for Scientific Research, Developmental Scientific Research, and Scientific Research on Priority Areas from the Ministry of Education, Science, Sports, and Culture, Takeda Medical Research Foundation, Uehara Memorial Foundation, grant-in-aid of The Japan Medical Association, The Kato Memorial Trust for Nambyo Research, Takeda Science Foundation, and a Japan Heart Foundation Research Grant. The costs of publication of this article were defrayed in part by the payment of page charges. This article must therefore be hereby marked "*advertisement*" in accordance with 18 U.S.C. Section 1734 solely to indicate this fact.

[S] The on-line version of this article (available at http://www.jbc.org) contains Supplementary Data.

** To whom correspondence should be addressed: Dept. of Cardiovascular Science and Medicine, Chiba University Graduate School of Medicine, 1-8-1 Inohana, Chuo-ku, Chiba 260-8670 Japan. Tel.: 81-43-226-2097; Fax: 81-43-226-2096; E-mail: komuro-tky@umin.ac.jp.

[1] The abbreviations used are: SP, side population; PE, phycoerythrin; PBS, phosphate-buffered saline; FBS, fetal bovine serum; MHC, myosin heavy chain; MLC, myosin light chain; MACS, Magnetic Cell Sorting; ALP, alkaline phosphatase; MEF, muscle enhancer factor.

This paper is available on line at http://www.jbc.org

TABLE I
PCR primers and PCR conditions

Primer	Product size	Annealing temperature
	bp	°C
α-MHC		
5′-GGAAGAGTGAGCGGCCATCAAGG-3′	302	65
5′-CTGCTGGAGAGGTTATTCCTCG-3′		
β-MHC		
5′-GCCAACACCAACCTGTCCAAGTTC-3′	205	66
5′-TGCAAAGGCTCCAGGTCTGAGGGC-3′		
MLC-2a		
5′-CAGACCTGAAGGAGACCT-3′	286	54
5′-GTCAGCGTAAACAGTTGC-3′		
MLC-2v		
5′-GCCAAGAAGCGGATAGAAGG-3′	499	55
5′-CTGTGGTTCAGGGCTCAGTC-3′		
Cardiac α-actin		
5′-CTGAGATGTCTCTCTCTCTTAG-3′	99	60
5′-ACAATGACTGATGAGAGATG-3′		
Csx/Nkx-2.5		
5′-CAGTGGAGCTGGACAAAGCC-3′	216	55
5′-TAGCGACGGTTCTGGAATTT-3′		
GATA4		
5′-CTGTCATCTCACTATGGGCA-3′	275	60
5′-CCAAGTCCGAGCAGGAATTT-3′		
MEF-2C		
5′-GGCCATGGTACACCGAGTACAACGAGC-3′	401	62
5′-GGGGATCCCTGTGTTACCTGCACTTGG-3′		
Oxytocin receptor		
5′-AAGATGACCTTCATCATTGTTC-3′	303	61
5′-CGACTCAGGACGAAGGTGGAGGA-3′		
ALP		
5′-TTGAAACTCCAAAAGCTCAACACCA-3′	450	62
5′-TCTCGTTATCCGAGTACCAGTCCC-3′		
Osteocalcin		
5′-CCGGGAGCAGTGTGAGCTTA-3′	92	62
5′-TAGATGCGTTTGTAGGCGGTC-3′		
β-Actin		
5′-GGACCTGGCTGGCCGGGACC-3′	583	60
5′-GCGGTGCACGATGGAGGGGC-3′		

(20). Although the precise mechanism of the effect of oxytocin is not clear, oxytocin may play an important role in the differentiation into cardiomyocytes from primitive cells including adult somatic stem cells. Here, we first report that a novel population from Sca-1+ cells derived from the adult murine heart proliferates and differentiates into beating cardiomyocytes with oxytocin treatment.

EXPERIMENTAL PROCEDURES

Animals and Reagents—Wild mice (C57Bl/6) were purchased from Takasugi Experimental Animals Supply, Co, LTD, Japan. All protocols were approved by the Institutional Animal Care and Use Committee of Chiba University. Phycoerythrin (PE) -conjugated anti-Sca-1 (anti-Ly6A/E), anti-c-kit (anti-CD117) antibodies were purchased from eBioscience (San Diego, CA). PE-conjugated anti-CD34, anti-CD45, and biotin-conjugated anti-Sca-1 antibodies were purchased from BD Pharmingen (San Diego, CA). The following antibodies were used for immunostaining: mouse monoclonal anti-cardiac troponin T (RV-C2, DSMZ-Deutsche Sammlung von Mikroorganismen und Zellkulturen GmbH, Germany), rabbit polyclonal anti-atrial natriuretic factor-1 (ANF) (Peninsula Laboratories, San Carlos. CA), goat polyclonal anti-GATA4 (Santa Cruz Biotechnology, Santa Cruz, CA), mouse monoclonal anti-myosin light chain-2v (MLC-2v) (BioCytex, France), mouse monoclonal anti-tropomyosin (Sigma Aldrich), mouse monoclonal anti-sarcomeric myosin heavy chain (MF-20) (American Type Culture Collection), rabbit polyclonal anti-connexin 43 (Zymed Laboratories, South San Francisco, CA). Fluorescent secondary antibodies were purchased from Jackson ImmunoResearch Laboratory (Bar Harbor, ME). Other reagents that are not specified were obtained from Sigma-Aldrich.

Isolation and Culture of Sca-1+ Cells from the Adult Murine Heart—A heart of adult C57Bl/6 mouse (10–12 weeks old) was enzymatically dissociated into a single cell suspension as described previously (21). Enrichment of Sca-1+ cells was achieved by sorting using the Magnetic Cell Sorting (MACS) system (Miltenyl Biotec, Sunnyvale, CA). Whole primary cell suspension was incubated with PE-conjugated anti-Sca-1 antibody for 10 min on ice, washed in PBS supplemented with 3% FBS, incubated with anti-PE micro beads for 15 min at 4 °C, and washed with PBS supplemented with 3% FBS. The samples were passed through a MACS column set up in a Miltenyl magnet and the Sca-1+ cells were eluted from the column by washing with PBS supplemented with 3% FBS. To increase the purity of the Sca-1+ cells, magnetic sorting was performed one more time. The Sca-1+ cells were cultured on 1% gelatin-coated dishes with Iscove's Modified Dulbecco's Medium (IMDM) supplemented with 10% FBS, 100 μg/ml of penicillin, and 250 μg/ml of streptomycin at 37 °C in humid air with 5% CO_2. Twenty-four hours after seeding, the cells were treated with 10 μM 5′-azacytizine for the initial 72 h or 100 nM oxytocin (WAKO, Japan). After treatment, the medium was changed every 3 days.

Characterization of Cardiac Muscle-derived Stem Cells for Flow Cytometric Analysis—Sca-1+ cells were isolated by the MACS system with biotin-conjugated anti-Sca-1 antibody and anti-biotin micro beads. Magnetic sorting was repeated twice, and the cells were incubated with PE-conjugated anti-CD45 antibody, PE-conjugated anti-CD34 antibody, and PE-conjugated anti-c-kit antibody, respectively for 10 min on ice and washed with PBS supplemented with 3% FBS. The percentages of CD45+, CD34+, and c-kit+ cells were analyzed by the EPICS ALTRA flow cytometer using EXPO32 software (Beckman Coulter, Miami, FL).

RNA Extraction and Reverse Transcriptase-PCR—Total RNA was extracted from the adult murine heart, liver, and Sca-1+ cells by RNA-bee reagent (TEL-TEST, Friendswood, TX). Reverse transcriptase (RT)-PCR of genes of cardiac transcription factors, including Csx/Nkx-2.5 (22), GATA4 (23), muscle enhancer factor-2C (MEF-2C) (24), and cardiac structural proteins, including α- and β-myosin heavy chain (MHC) (25), myosin light chain-2a (MLC-2a), MLC-2v (26), cardiac α-actin (27), and oxytocin receptor (19), alkaline phosphatase (28), osteocalcin (29) were performed using 0.1 μg of total RNA. β-actin (30) was used as an internal control. The primers used in this study and PCR conditions are described in Table I. The PCR products were size-fractionated by 2% agarose gel electrophoresis.

Immunocytochemistry—Cells were fixed with 4% paraformaldehyde for 15 min at room temperature. After preblocking with PBS containing 2% donkey serum, 2% bovine serum albumin and 0.2% Nonidet P-40 for

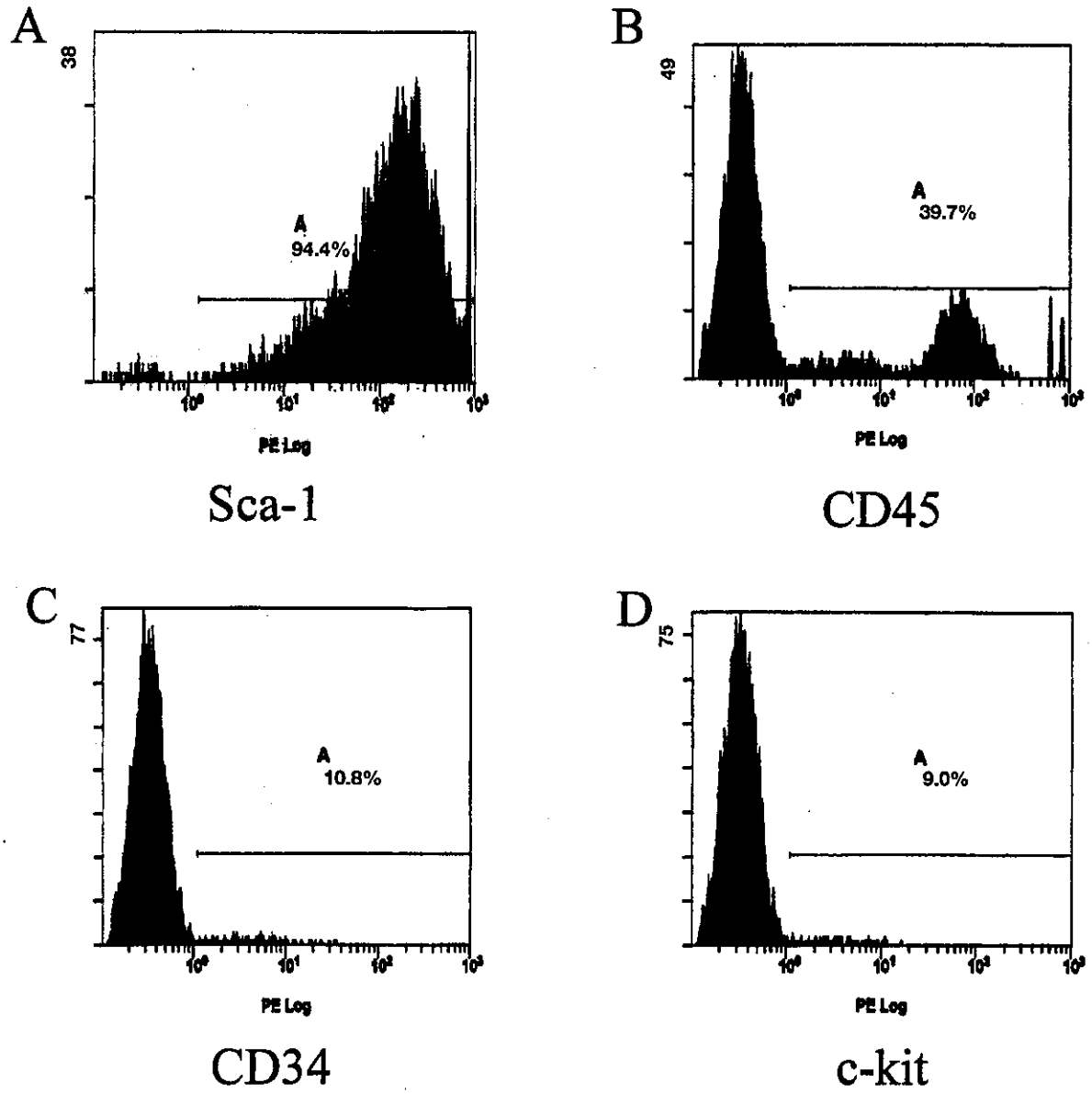

FIG. 1. **Flow cytometric analysis of Sca-1+ cells.** Sca-1+ cells were enriched by the MACS system with PE-conjugated anti-Sca-1 antibody and anti-PE micro beads, and after sorting twice, ~90% of the cells expressed Sca-1 (*A*). Sca-1+ cells were stained with PE-conjugated anti-CD45 antibody, anti-CD34 antibody, and anti-c-kit antibody. In enriched Sca-1+ cells, ~40% of the cells expressed CD45 (*B*), ~10% of the cells expressed CD34 (*C*), and c-kit (*D*).

30 min, primary antibodies in PBS containing 2% donkey serum, 2% bovine serum albumin and 0.1% Nonidet P-40 were applied overnight in 4 °C. Subsequently cells were washed three times in PBS, and then fluorescein isothiocyanate- or Cy5-conjugated secondary antibodies were applied to visualize expression of specific proteins. Nuclear staining was performed with TO-PRO-3 (Molecular Probes, Eugene, OR). Images of cells were taken by laser confocal microscopy (Radiance2000, Bio-Rad, Hercules, CA).

Phase Contrast Live Imaging—Live images were taken by a Zeiss inverted microscope (Carl Zeiss, Jena, Germany) equipped with phase-contrast objectives and an AxioCam camera. Live image of beating cells were obtained by a chilled CCD camera (Hamamatsu) using I-O DATA Videorecorder software.

Measurement of Intracellular Ca^{2+} Concentration—Intracellular Ca^{2+} concentration ($[Ca^{2+}]_i$) in beating cells derived from cardiac Sca-1+ cells was measured as previously described (31). The beating cells on gelatin-coated glass coverslips were incubated in HEPES (loading) solution containing 1 μM fluo 3-acetoxymethyl ester (fluo 3-AM; Molecular Probes) at 36 °C in the dark for 30 min. The loading solution was prepared by diluting a 100 μM fluo 3 stock solution, which contained 0.45% Pluronic F127 (Molecular Probes), 10% dimethyl sulfoxide, and 90% FBS. HEPES solution consisted of (in mM) 126 NaCl, 4.4 KCl, 1.0 $MgCl_2$, 1.08 $CaCl_2$, 24 HEPES, 13 NaOH, 11 glucose, and 0.5 probenecid (pH 7.4). The coverslips were washed twice with dye-free HEPES solution and placed in a flow-through chamber on the microscope. Fluo 3-loaded beating cells were excited by 480-nm light and emitted fluorescence was recorded at 530 nm by a photomultiplier tube (AIM-10, InterMedical, Co, Japan) and digitized (PowerLab 2/20, AD-instruments, Castle Hill, Australia). Curve fits were performed with Origin 7J software (MicroCal Software, Northampton, MA). The intensity of the fluorescence at 530 nm increased with an increase in $[Ca^{2+}]_i$.

Estimation of Pluripotency—Osteogenic differentiation of Sca-1+ cells from the adult murine heart was induced in IMDM supplemented with 10% FBS, 50 μM ascorbic acid 2-phosphate, 0.1 μM dexamethasone, and 10

mM β-glycerophosphate as described previously (32). For detection of osteocytes, alkaline phosphatase staining (leukocyte alkaline phosphatase assay kit, Sigma-Aldrich) was used. Adipogenic differentiation was induced as described previously (28). Briefly the cells were cultured with Dulbecco's Modified Eagle's Medium (DMEM) supplemented with 5% horse serum with MDI-I mixture; 0.5 mM methyl-isobutylxanthine, 1 μM dexamethasone, 100 mM indomethacin, and 10 μg/ml insulin for 2 days and then cultured with Dulbecco's modified Eagle's medium supplemented with 5% horse serum and 10 μg/ml of insulin for 1 day. Treatment with MDI-I followed by insulin was repeated four times. For detection of accumulated oil droplets, Oil-Red O staining was performed followed by nuclear hematoxylin counterstaining.

Statistical Analysis—Values are presented as mean ± S.E. The significance of differences among mean values was determined by analysis of variance. The accepted level of significance was $p < 0.05$.

RESULTS

Cell Surface Antigens of Sca-1+ Cells Derived from the Adult Murine Heart—Flow cytometric analysis revealed that Sca-1+ cells were enriched to over 90% when adult murine cardiac cells were sorted twice with the MACS system using PE-conjugated anti-Sca-1 antibody and anti-PE micro beads (Fig. 1*A*). The number of purified Sca-1+ cells was ~1×10^4 cells. Limana *et al.* (33) have estimated the number of cardiomyocytes in an adult murine heart as ~3×10^6. Therefore the percentage of cardiac Sca-1+ cells was ~0.3% of the total number of cardiomyocytes. Next we examined other cell surface antigens such as CD45, CD34, and c-kit in Sca-1+ cells. After repeated magnetic sorting with biotin-conjugated anti-Sca-1 antibody and anti-biotin micro beads, enriched Sca-1+ cells were incubated with PE-conjugated anti-CD45, CD34 and c-kit antibodies and analyzed by flow cytometry. In enriched Sca-1+ cells, ~40% of the cells expressed CD45 (Fig. 1*B*), and ~10% of the cells expressed CD34 (Fig. 1*C*) and c-kit (Fig. 1*D*).

Sca-1+ Cells from the Adult Murine Heart Differentiate into Beating Cardiomyocytes—In order to induce differentiation into cardiomyocytes, Sca-1+ cells were treated with either 5′-azacytizine or oxytocin. When Sca-1+ cells were cultured with medium containing FBS, they showed various cell shapes, and spindle-like and elongated shapes were predominant (Fig. 2*A*). Two weeks after treatment with oxytocin, small round cells with prominent nucleus and little cytoplasm appeared (*arrowheads* in Fig. 2*B*). These round cells rapidly proliferated, formed clusters, and detached from the culture dish so that spindle-shaped cells were left. The cells were re-plated when reached to confluence. Four weeks after starting treatment with oxytocin, some spontaneously beating cells were recognized among spindle-shaped cells (*arrow* in Fig. 2, *C* and *D* and Supplemental Data). Spontaneous beating was observed at ~1% cells. On the other hand, cells after treatment with 5′-azacytizine or vehicles showed fibroblast-like morphology, and never exhibited round or spindle-shaped morphology, or spontaneous beating.

Next we examined the gene expression of cardiac transcription factors and cardiac structural proteins in Sca-1+ cells by RT-PCR. Before treatment with 5′-azacytizine or oxytocin, only Csx/Nkx-2.5 and GATA4 were slightly expressed (Fig. 3, *lane P*). Four weeks after treatment with 5′-azacytizine or oxytocin, all genes of cardiac transcription factors including Csx/Nkx-2.5, GATA4, and MEF-2C and structural proteins such as α- and β-MHC, MLC-2a, MLC-2v, and cardiac α-actin were expressed (Fig. 3, *lane A* for 5′-azacytizine and *lane OT* for oxytocin). Treatment with 100 nM oxytocin antagonist (OTA, [d(CH_2)$_5$-1,Tyr(Me)-2,Thr-4,Orn-8,Tyr-NH_2-9] vasotocin, Wako, Japan) completely inhibited oxytocin-induced expression of cardiac genes (Fig. 3, *lane OT+OTA*). Total RNA obtained from the adult murine heart and liver were used as positive and negative controls (Fig. 3, *lane H* for heart and *lane L* for liver). Loading of equal amounts of RNA was confirmed by expression of the β-actin gene. Cardiac gene expression was not observed in cells cultured with vehicle (Fig. 3, *lane V*).

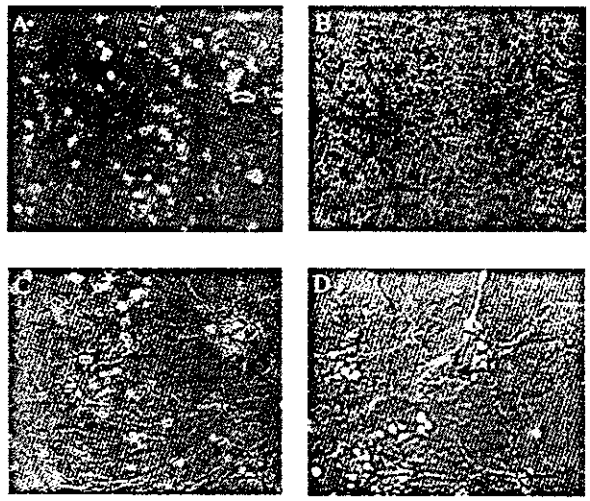

FIG. 2. **Phase contrast images of Sca-1+ cells before and after oxytocin treatment.** *A*, Sca-1+ cells before oxytocin treatment show small spindle-shaped morphology (0 weeks). *B*, two weeks after treatment with oxytocin, small round cells (*arrowheads*) have appeared. These round cells rapidly proliferated, formed clusters, and detached from the culture dish so that spindle-shaped cells were left. The cells were re-plated when reached to confluence. Four weeks after starting treatment with oxytocin, some spontaneously beating cells (*arrow* in *C* and *D*) were recognized among the spindle-shaped cells (*C*). *D*, magnified scale of the figure in *C*. *Bars*, 100 μM.

To examine the expression and localization of cardiac proteins, the Sca-1+ cells treated with oxytocin and 5′-azacytizine were stained with specific antibodies against cardiac proteins. The cells treated with oxytocin expressed GATA4 (Fig. 4*A*), ANF (Fig. 4*B*), and cardiac troponin T (Fig. 4, *A* and *B*). MLC-2v (Fig. 4*C*), sarcomeric myosin heavy chain (Fig. 4*D*), and tropomyosin (data not shown) were also expressed. Notably, staining of each contractile protein showed a fine striated pattern. Connexin 43 was expressed at the junction between two cardiac troponin T-expressing cells (Fig. 4*E*). These findings indicate that treatment with oxytocin induced differentiation of Sca-1+ cells, derived from the adult murine heart, into mature cardiomyocytes, which had well-organized structures and electrical junctions. After treatment with 5′-azacytizine, a fraction of cells expressed sarcomeric myosin heavy chain in fibrillar pattern (Fig. 4*F*), but not cardiac troponin T (data not shown). Next we sorted cardiac Sca-1+ cells on the basis of CD45 expression and cultured with oxytocin. Some of the Sca-1+/CD45− cells expressed sarcomeric myosin after oxytocin treatment, but none of the Sca-1+/CD45+ cells expressed myosin (data not shown), suggesting that Sca-1+ cells that can differentiate into cardiomyocytes are in CD45− population.

Cardiac contraction is regulated by beat to beat change in $[Ca^{2+}]_i$. To ascertain that the spontaneous beating of differentiated cardiac Sca-1+ cells depends on intracellular level of Ca^{2+}, we analyzed $[Ca^{2+}]_i$ transients of the beating cells. As shown in the *upper panel* of Fig. 5*A*, the spontaneous beating of differentiated Sca-1+ cells was accompanied with $[Ca^{2+}]_i$ transients. After treatment with 10^{-7} M isoproterenol for 5 min, the frequency of $[Ca^{2+}]_i$ transients was increased in comparison with control (Fig. 5*A*, *upper panel versus lower panel*). Next we examined the predominant subtype of β receptors, which mediates changes in beating rate. Differentiated cardiac Sca-1+ cells were treated with vehicle (PBS), propranolol, CGP20712A (β_1-selective blocker), or ICI118551 (β_2-selective blocker) for 30

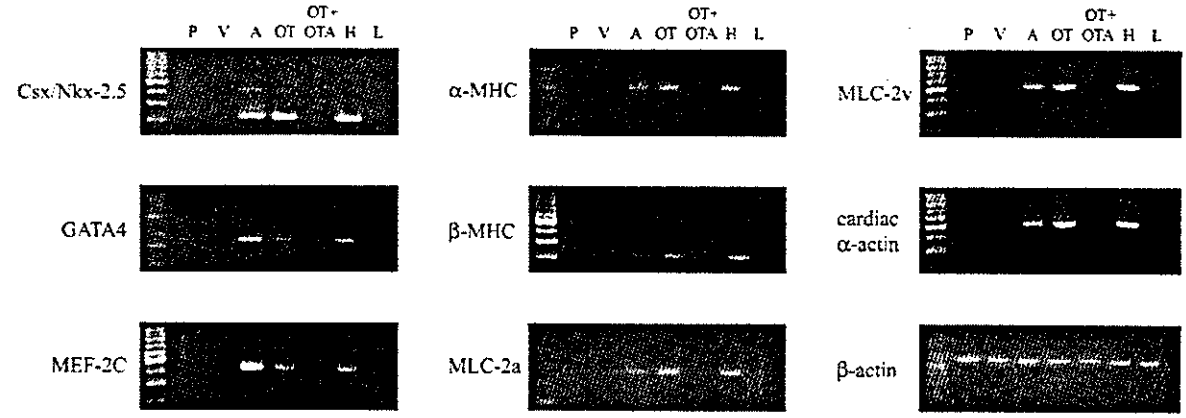

FIG. 3. **RT-PCR analysis of cardiac genes.** Sca-1+ cells after treatment with oxytocin (*lane OT*) or 5′-azacytizine (*lane A*) expressed Csx/Nkx-2.5, GATA4, MEF-2C, α-MHC, β-MHC, MLC-2a, MLC-2v, and cardiac α-actin. Although Sca-1+ cells before treatment (*lane P*) expressed Csx/Nkx-2.5 and GATA4 slightly, none of cells after treatment with vehicles (*lane V*) or oxytocin antagonist combined with oxytocin (*lane OT+OTA*) expressed any cardiac transcription factors. Heart (*lane H*) and liver (*lane L*) were used as positive and negative controls, respectively.

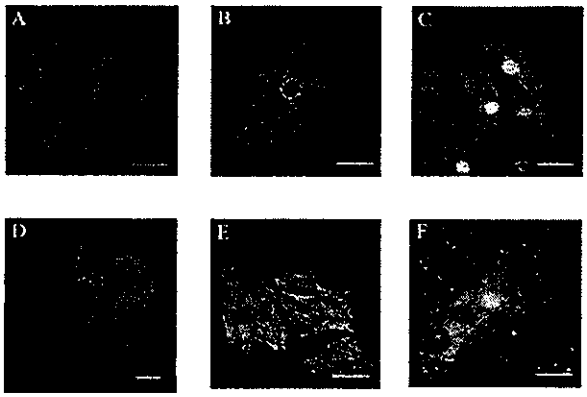

FIG. 4. **Immunocytochemical analysis of cardiac proteins.** *A–E*, cardiac differentiation of Sca-1+ cells after oxytocin treatment. Cells were double-stained using anti-GATA4 antibody (*A, green*), anti-ANF antibody (*B, green*), and anti-cardiac troponin T antibody (*A* and *B, blue*). Cells were stained with anti-MLC-2v (*C, green*) and anti-sarcomeric myosin heavy chain antibodies (*D, green*), and nuclei were stained with TO-PRO-3 (*C* and *D, blue*). Cells were double-stained using anti-cardiac troponin T antibody (*E, green*) and anti-connexin 43 antibody (*E, blue*). *F*, differentiation of Sca-1+ cells after 5′-azacytizine treatment. Cells were stained with anti-sarcomeric myosin heavy chain (*F, green*) and TO-PRO-3 (*F, blue*). *Bars*, 50 μm.

min and then stimulated with isoproterenol alone for 5 min. Isoproterenol significantly increased the beating rate of the control cells (control: 131.9 ± 5.6, $n = 10$ *versus* isoproterenol: 228.9 ± 7.3, $n = 10$, $p < 0.01$, Fig. 5*B*). The pretreatment with propranolol (average 196.4 ± 5.6, $n = 10$, $p < 0.05$ *versus* isoproterenol) and CGP20712A (average 188.9 ± 7.5, $n = 10$, $p < 0.05$ *versus* isoproterenol) reduced the increase in beating rate in response to isoproterenol significantly (Fig. 5*B*). ICI118551 had no effect on the isoproterenol-induced increase in beating rate.

Sca-1+ Cells from the Adult Murine Heart Express Oxytocin Receptor mRNA—To elucidate the role of oxytocin receptor in cardiomyogenesis of Sca-1+ cells, we examined the expression of oxytocin receptor in Sca-1+ cells. Oxytocin receptor mRNA was present at low levels in Sca-1+ cells before oxytocin treatment (Fig. 6, *lane P*). Expression levels of oxytocin receptor remained low in cells cultured with vehicle (Fig. 6, *lane V*). After treatment with oxytocin, expression levels of oxytocin receptor were up-regulated (Fig. 6, *lane OT*). In accordance with the inhibitory effect of oxytocin antagonist on oxytocin-induced cardiac differentiation, oxytocin antagonist inhibited oxytocin-induced up-regulation of the oxytocin receptor (Fig. 6, *lane OT+OTA*). These results suggest that the positive feedback mechanism, namely oxytocin-induced up-regulation of oxytocin receptor, plays an important role in oxytocin-induced cardiomyocyte differentiation of cardiac Sca-1+ cells.

Sca-1+ Cells Can Differentiate into Osteocytes and Adipocytes—It has been reported that Sca-1+ cells from skeletal muscle and bone marrow differentiate into various types of cells such as adipocytes, endothelial cells, muscle, neural, and hepatic cells (9, 11, 14). To determine whether the Sca-1+ cells from the adult murine heart have pluripotency, we examined whether these cells could differentiate into cells other than cardiomyocytes. When treated with osteogenic inducers, some of Sca-1+ cells were stained with alkaline phosphatase, one of the early markers of osteogenesis (Fig. 7*A*). RT-PCR clearly revealed that osteogenic marker mRNAs such as alkaline phosphatase and osteocalcin were induced in Sca-1+ cells after treatment with osteogenic inducers (Fig. 7*B*). On the other hand, Sca-1+ cells treated with oxytocin never expressed alkaline phosphatase and osteocalcin. When Sca-1+ cells were cultured with MDI-I mixture for twelve days, some of Sca-1+ cells showed cytoplasmic accumulation of oil droplets stained with Oil-Red O, indicating that Sca-1+ cells differentiated into adipocytes (Fig. 7*C*).

DISCUSSION

In this report, we have first demonstrated that adult cardiac Sca-1+ cells can differentiate into beating cardiomyocytes *in vitro* by treatment with oxytocin. When treated with oxytocin, the Sca-1+ cells expressed cardiac genes including Csx/Nkx-2.5, GATA4, MEF-2C, α-MHC, β-MHC, MLC-2a, MLC-2v, and cardiac α-actin, and cardiac proteins including GATA4, cardiac troponin T, tropomyosin, MLC-2v, sarcomeric myosin heavy chain, ANF, and connexin 43. Furthermore, some of Sca-1+ cells showed well organized sarcomere and spontaneous beating. Although transient treatment with 5′-azacytizine also induced expression of cardiac genes in Sca-1+ cells, it did not induce expression of cardiac troponin T, assembly of sarcomere or spontaneous beating. These results suggest that treatment with 5′-azacytizine induces differentiation of Sca-1+ cells into cardiomyocytes incompletely and that oxytocin is a more potent inducer of cardiac differentiation than 5′-azacytizine.

P19 teratocarcinoma cells differentiate into beating cardiomyocytes after treatment with Me_2SO and have been considered as a good model of *in vitro* cardiogenesis (34, 35). Several

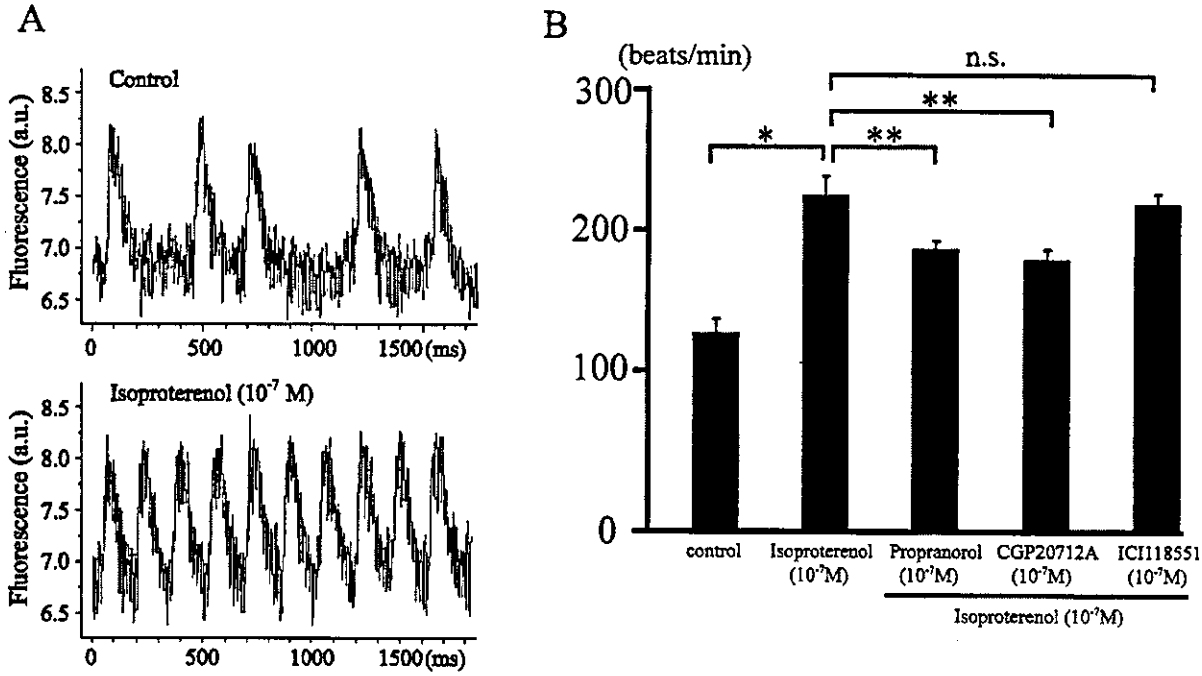

FIG. 5. **Physiological analysis of differentiated cardiac Sca-1+ cells.** *A*, $[Ca^{2+}]_i$ transients of beating cells derived from cardiac Sca-1+ cells before (*upper panel*) and after (*lower panel*) treatment with isoproterenol. *B*, the effects of subtype-specific β receptor blockers on isoproterenol-induced increase in beating rate of differentiated cardiac Sca-1+ cells. Preincubation with 10^{-7} M propranolol (nonselective β blocker) and 10^{-7} M CGP20712A (β_1-selective blocker) reduced isoproterenol-induced increase in beating rate significantly but 10^{-7} M ICI118551 (β_2-selective blocker) did not. *, $p < 0.01$ *versus* control; **, $p < 0.05$ *versus* isoproterenol only; *n.s.*, not significant.

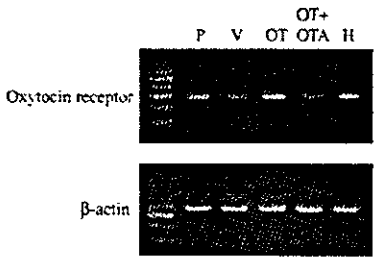

FIG. 6. **RT-PCR analysis of oxytocin receptor expression in Sca-1+ cells.** Oxytocin receptor mRNA was present at low levels in Sca-1+ cells before treatment (*lane P*). After oxytocin treatment, the oxytocin receptor mRNA expression was up-regulated (*lane OT*), but oxytocin antagonist inhibited oxytocin-induced oxytocin receptor up-regulation (*lane OT+OTA*).

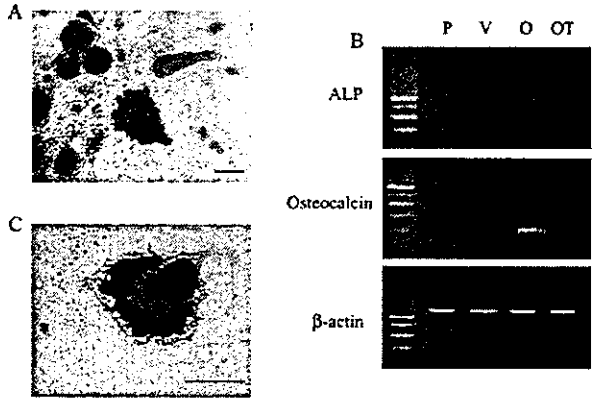

FIG. 7. **Osteogenic and adipogenic differentiation potential of Sca-1+ cells derived from the adult murine heart.** *A*, osteogenic differentiation of Sca-1+ cells was induced by treatment with ascorbic acid 2-phosphate, dexamethasone, and β-glycerophosphate for 3 weeks. Alkaline phosphatase staining (*blue*) was used for detection of osteocytes. *B*, RT-PCR experiment clearly revealed that osteogenic marker mRNAs such as alkaline phosphatase (*ALP*) and osteocalcin were induced in Sca-1+ cells by treatment with osteogenic inducers (*lane P* for pretreatment, *lane V* for vehicle treatment, *lane O* for osteogenic induction). Sca-1+ cells treated with oxytocin never expressed osteogenic marker mRNAs (*lane OT* for oxytocin treatment). β-actin was used as an internal control. *C*, adipogenic differentiation of Sca-1+ cells was induced by treatment with adipogenic mixture (MDI-I) for twelve days. Oil-Red O staining showed adipogenic differentiation of Sca-1+ cells. Hematoxylin was used for counterstaining of nuclei. *Bars*, 50 μm.

essential transcription factors in cardiomyogenesis such as GATA4 (34), Csx/Nkx-2.5 (34), and MEF-2C (36) are up-regulated in P19 cells treated with Me_2SO. Recently Paquin *et al.* (19) have reported that oxytocin induces P19 embryonic carcinoma cells to differentiate into cardiomyocytes. Treatment with oxytocin as well as with Me_2SO induced colony formation of beating cardiomyocytes, expression of cardiac proteins, and oxytocin receptor proteins. In this study, cardiac Sca-1+ cells expressed low levels of oxytocin receptor mRNA that were positively regulated by oxytocin itself, and pretreatment with oxytocin antagonist completely inhibited oxytocin-induced expression of cardiac genes. These results suggest that oxytocin induces cardiomyocyte differentiation of cardiac Sca-1+ cells through oxytocin receptors. Furthermore Sca-1+ cells treated with oxytocin did not express osteogenic marker mRNAs, suggesting that oxytocin is not a nonspecific inducer like 5'-azacytizine but has some specificity for cardiac lineage.

Oxytocin receptors are coupled to $G_{q/11}$ class GTP-binding proteins and stimulate the generation of inositol trisphosphate and diacylglycerol, leading to Ca^{2+} release and activation of protein kinase C (37). Oxytocin stimulates cell proliferation through calcium (38, 39) and protein kinase C pathways (38). Cassoni *et al.* (40) have reported that oxytocin stimulates cell

proliferation through oxytocin receptors that lead to an increase in intracellular Ca^{2+} and tyrosine phosphorylation. Tyrosine phosphorylation in oxytocin signaling has been reported to activate both p38 mitogen-activated protein kinase and extracellular signal-regulated kinase 2 (41, 42). The mechanism by which oxytocin stimulates tyrosine phosphorylation has not been elucidated, but may be mediated by $G\beta\gamma$ subunit dissociating from G_α subunit. Oxytocin inhibits the proliferation of human brain tumors (43), breast cancer cells (44), and adenocarcinoma of endometrium (45) via the cyclic adenosine monophosphate-protein kinase A pathway. Tahara *et al.* (46) have reported that the RhoA/Rho-kinase cascade is involved in oxytocin-induced rat uterine contraction. Among the considerable diversity of oxytocin-mediated signaling pathways, the specific pathway that activates cardiogenesis is currently unknown. Recently post-translational modification of cardiac transcription factors has been reported to be important for their transcriptional activities. Rho-like GTPases can phosphorylate GATA4 via activation of the p38 mitogen-activated protein kinase pathway, which enhances the potency of GATA4 (47). MEF2 is stimulated by calmodulin kinase activation in the heart (48). It remains to be determined which oxytocin signaling pathways are important for differentiation of cardiomyocytes.

It has been reported that c-kit+, Sca-1+, lineage-, and CD34-/low fraction of bone marrow cells contain hematopoietic stem cells, which contribute to long term multilineage reconstitution of the blood system in mice (49). Orlic *et al.* (50) and Gojo *et al.* (10) have reported that c-kit+ bone marrow cells and c-kit+ bone marrow-derived mesenchymal cells transdifferentiate into cardiomyocytes *in vivo*, suggesting that c-kit is one of the cell surface markers of multipotent stem cells in bone marrow. The multipotential stem cells also reside in skeletal muscle, although the origin of the stem cells is still controversial (51). Skeletal muscle-derived stem cells reported by Qu-Petersen *et al.* (11) and Torrente *et al.* (13) highly express CD34 and Sca-1 but not c-kit and CD45 and differentiate into neural and endothelial cells. In our study, cardiac Sca-1+ cells expressed low levels of c-kit, suggesting that the features of stem cell markers on cardiac stem cells is distinct from bone marrow-derived stem cells and rather similar to skeletal muscle-derived stem cells.

Tamaki *et al.* (14) isolated CD34+ and CD45− cells from the interstitial space of skeletal muscle, which highly expressed Sca-1 but not other endothelial progenitor cell markers. The CD34+/CD45− cells differentiated into adipocytes, endothelial and myogenic cells and expressed Bcrp1/ABCG2 gene mRNA, which is an important determinant of the SP phenotype. Recently Polesskaya *et al.* (52) have reported that CD45+/Sca-1+ cells from injured skeletal muscle differentiate into myoblasts much more than CD45−/Sca-1 cells. Because of the hematopoietic restricted expression of CD45 antigen, skeletal myogenic CD45+/Sca-1+ cells might be of hematopoietic origin. In our study, cardiac Sca-1+ cells expressed low levels of CD34 and ~40% of the cardiac Sca-1+ cells expressed CD45, one of hematopoietic cell markers. We sorted cardiac Sca-1+ cells on the basis of CD45 expression and cultured them with oxytocin. Some Sca-1+/CD45− cells expressed sarcomeric myosin after oxytocin treatment, but no Sca-1+/CD45+ cells expressed myosin (data not shown), suggesting that Sca-1+ cells that can differentiate into cardiomyocytes are in the CD45− population. Therefore, in terms of the expression of CD34 and CD45, the cardiac muscle stem cells are distinct from the previously reported skeletal muscle-derived stem cells.

Sca-1+ cells from the adult heart expressed GATA4 and Csx/Nkx-2.5, but not Oct-3/4 before treatment with oxytocin (data not shown), suggesting that the Sca-1+ cells are committed to cardiomyocytes to some degree. Makino *et al.* (24) have reported that mouse bone marrow-derived mesenchymal stem cells (CMG cells) differentiate into cardiomyocyte after 5′-azacytizine treatment. Although the cell surface antigens of CMG cells were not analyzed, the bone marrow-derived mesenchymal stem cells, which differentiated into cardiomyocytes after 5′-azacytizine treatment *in vivo*, expressed Sca-1, c-kit, and CD34 (10), suggesting that the cardiac Sca-1+ cells are different from bone marrow-derived mesenchymal stem cells. Cardiac Sca-1+ cells differentiated into osteocytes and adipocytes in appropriate conditions, suggesting that cardiac Sca-1+ cells have the intragerm layer multipotency. It remains to be determined whether the cardiac Sca-1+ cell population contains stem cells capable of differentiating to extra germ layer lineage.

The spontaneously beating differentiated cardiac Sca-1+ cells showed $[Ca^{2+}]_i$ transients and treatment with isoproterenol increased the frequency of $[Ca^{2+}]_i$ transients and beating rate. The similar response to isoproterenol has been reported in adult murine cardiomyocytes (53), embryonic stem cells-derived cardiomyocytes (54), and CMG cells (55). The β_1-selective blocker, CGP20712A, significantly reduced isoproterenol-induced increase in beating rate to the same extent as the non-selective β-blocker, propranolol, but the β_2-selective blocker, ICI118551, did not. These results suggest that the β_1 receptor is the predominant subtype that mediates the changes in beating rate of cardiomyocytes derived from Sca-1+ cells.

During the preparation of this article, two studies on cardiac stem cells were reported (56, 57). They have shown that c-kit+ or Sca-1+ cells derived from the adult murine heart express cardiac genes and proteins after the cardiogenic induction. We showed for the first time that there are potential adult cardiac stem cells that have an ability to proliferate and differentiate into various types of cells including beating cardiomyocytes *in vitro*. Although the role of cardiac stem cells is uncertain, our results suggest their possible role in cardiac repair. In addition, the understanding of precise molecular mechanisms of the differentiating process of cultured cardiac stem cells may provide us with new insights into cardiac development and regeneration.

Acknowledgments—We thank A. Ohkubo, R. Kobayashi, E. Fujita, M. Watanabe, M. Iida, and Y. Ohtsuki for technical assistance.

REFERENCES

1. Kajstura, J., Leri, A., Finato, N., Di Loreto, C., Beltrami, C. A., and Anversa, P. (1998) *Proc. Natl. Acad. Sci. U. S. A.* **95**, 8801–8805
2. Leri, A., Barlucchi, L., Limana, F., Deptala, A., Darzynkiewicz, Z., Hintze, T. H., Kajstura, J., Nadal-Ginard, B., and Anversa, P. (2001) *Proc. Natl. Acad. Sci. U. S. A.* **98**, 8626–8631
3. Beltrami, A. P., Urbanek, K., Kajstura, J., Yan, S. M., Finato, N., Bussani, R., Nadal-Ginard, B., Silvestri, F., Leri, A., Beltrami, C. A., and Anversa, P. (2001) *N. Eng. J. Med.* **344**, 1750–1757
4. Quaini, F., Urbanek, K., Beltrami, A. P., Finato, N., Beltrami, C. A., Nadal-Ginard, B., Kajstura, J., Leri, A., and Anversa, P. (2002) *N. Eng. J. Med.* **346**, 5–15
5. Anversa, P., and Nadal-Ginard, B. (2002) *Nature* **415**, 240–243
6. Asakura, A., and Rudnicki, M. A. (2002) *Exp. Hematol.* **30**, 1339–1345
7. Hierlihy, A. M., Seale, P., Lobe, C. G., Rudnicki, M. A., and Megeney, L. A. (2002) *FEBS Lett.* **530**, 239–243
8. van der Rijn, M., Heimfeld, S., Spangruade, G. J., and Wiessman, I. L. (1989) *Proc. Natl. Acad. Sci. U. S. A.* **86**, 4634–4638
9. Okumoto, K., Saito, T., Hattori, E., Ito, J. I., Adachi, T., Takeda, T., Sugahara, K., Watanabe, H., Saito, K., Togashi, H., and Kawata, S. (2003) *Biochem. Biophys. Res. Commun.* **304**, 691–695
10. Gojo, S., Gojo, N., Takeda, Y., Mori, T., Abe, H., Kyo, S., Hata, J., and Umezawa, A. (2003) *Exp. Cell Res.* **288**, 51–59
11. Qu-Petersen, Z., Deasy, B., Jankowski, R., Ikezawa, M., Cummins, J., Pruchnic, R., Mytinger, J., Cao, B., Gates, C., Wernig, A., and Huard, J. (2002) *J. Cell Biol.* **157**, 851–864
12. Asakura, A., Seale, P., Girgis-Gabardo, A., and Rudnicki, M. A. (2002) *J. Cell Biol.* **159**, 123–134
13. Torrente, Y., Tremblay, J. P., Pisati, F., Belicchi, M., Rossi, B., Sironi, M., Fortunato, F., El Fahime, M., D'Angelo, M. G., Caron, N. J., Constantin, G., Paulin, D., Scarlato, G., and Bresolin, N. (2001) *J. Cell Biol.* **152**, 335–348